arXiv:astro-ph/0308333v1 19 Aug 2003

Draft: February 2, 2008

Meeting the Cool Neighbours, VI: A search for nearby ultracool dwarfs in the Galactic Plane

I. Neill Reid

Space Telescope Science Institute, 3700 San Martin Drive, Baltimore, MD 21218
and
Department of Physics and Astronomy, University of Pennsylvania, 209 South 33rd Street, Philadelphia, PA 19104

inr@stsci.edu

ABSTRACT

Surveys for nearby low-luminosity dwarfs tend to avoid the crowded regions of the Galactic Plane. We have devised near-infrared colour-magnitude and colour-colour selection criteria designed to identify late-type M and early-type L dwarfs within 12 parsecs of the Sun. We use those criteria to search for candidates within the regions of the Galactic Plane ($|b| < 10^o$) covered by the Second Incremental Release of data from the Two-Micron All Sky Survey. Detailed inspection of the available photographic images of the resulting 1299 candidates confirms only two as ultracool dwarfs. Both are known proper motion stars, identified in the recent survey by Lépine *et al.*(2002). Despite the low numbers, the inferred surface density is consistent with comparable surveys at higher latitudes. We discuss the implications for the luminosity function, and consider means of improving the efficiency and scope of photometric surveys in the Plane.

Subject headings: stars: low-mass, brown dwarfs; stars: luminosity function, mass function; Galaxy: stellar content

1. Introduction

Most of the stellar systems known to lie within the immediate Solar Neighbourhood were identified originally in proper motion surveys, notably Willem Luyten's analyses of photographic plates taken with Palomar 48-inch Schmidt (Luyten, 1979; 1980, and references

therein). The high star densities present near the Galactic Plane have long been recognised as a hindrance to that type of survey, particularly in searches for stars of intrinsically low luminosity. Thus, while analysis of current nearby-star catalogues, such as the preliminary Third Nearby Star Catalogue (Gliese & Jahreiss, 1991: pCNS3), shows no evidence for bias at low Galactic latitudes in the distribution of early- and mid-type M dwarfs, there is a clear deficit of later-type (spectral types $\geq$ M5) dwarfs (Reid *et al.*, 2002a: PMSU4). This deficiency has been highlighted by Lépine *et al.*'s (2002) recent proper motion survey of the northern Galactic Plane, which uses image subtraction to compare scans of first- and second-epoch sky survey plates. Of the 601 stars identified in that survey with $\mu > 0.5''$ yr^{-1} , only 460 are included in the Luyten Half Second (LHS) catalogue (Luyten, 1980), even though all are visible on plate material taken for the first Palomar Sky Survey (POSS I).

Photometric surveys provide a complementary and, in some cases, more effective means of surveying the Galactic Plane for nearby, late-type dwarfs. Proper motion surveys require detection at several epochs, and searches for faint red stars are often limited by the availability of only blue-sensitive imaging data at early epochs. Photometric surveys can be tuned to the longer wavelengths where low-mass dwarfs are most luminous, and can avoid the (often exagerated) potential for kinematic bias inherent in proper motion selection. In practice, most surveys use both techniqes, either using photometry or spectroscopy to confirm proper-motion selected candidates or, as described further below, using proper motion to identify nearby dwarfs in a photometrically-selected sample.

To be most effective, photometric surveys should span a wide wavelength range, with near-contemporary observations in the various passbands. The latter attribute is necessary to allow reliable matching of separate observations of stars with sensible proper motions; the former is required since other sources, such as distant giants, reddened stars and young T Tauri stars, can mimic M dwarf colours in some passbands, and those contaminants greatly outnumber genuine nearby stars at low latitudes. Unfortunately, at present we lack the full complement of such surveys. The Two-Micron All-Sky Survey (2MASS: Skrutskie *et al.*, 1997) provides high quality astrometry and photometry at near-infrared wavelengths, and far-red I-band data are now available for almost the full sky, through the second generation UK Schmidt and POSS II surveys (Reid *et al.*, 1991). Scans of the latter plates can provide astrometrically accurate data for well-resolved sources, with photometric uncertainties of $\pm$0.25 magnitudes to I$\sim$ 18.5 magnitudes. However, published optical catalogues based on Schmidt surveys (e.g. USNO-A2 catalogue, Monet *et al.*, 1998) generally require detection in two or more passbands. As a result, M-dwarf surveys are often limited by the sensitivity of the blue-passband 103aO or IIIaJ survey plates.

Given these technical constraints, our initial survey for previously-undetected ultracool

dwarfs in the immediate Solar Neighbourhood (d < 20 pc) was limited to $|b| > 10^o$, where infrared data alone suffice (Cruz *et al.*, 2003; Paper V). This paper outlines our first attempt to extend that survey to lower latitudes, albeit for a more restricted range of distance and spectral type. Section 2 outlines our selection criteria; section 3 describes our results; section 4 discusses the nature of the faint proper motion stars identified recently by Lépine *et al.*(2002); and section 5 presents our conclusions.

2. Selection Criteria

We use 2MASS near-infrared photometry as the basis for the initial selection of candidate ultracool dwarfs (spectral types later than M7). The 2MASS Second Incremental Data Release (hereinafter referred to as the 2M2nd) covers 48% of the sky, including $\sim 7\%$ within 10 degrees of the Galactic Plane. As discussed in Paper V, and illustrated in Figure 1, (J-K_S) colours provide a means of identifying late-type M and L dwarfs, and deriving moderately-accurate photometric parallaxes. At high galactic latitude, we used J magnitudes and JHK colours to isolate ~ 2000 objects with photometric properties consistent with dwarfs within 20-parsecs of the Sun (the 2MU2 sample). Unfortunately, those criteria fail at lower latitudes: nearly 1 million sources with $|b| < 10^o$ meet the colour/magnitude criteria outlined in Paper V. Clearly, it is not possible to carry out the same kind of detailed follow-up observations for such a large sample, so we have adopted different tactics in our low-latitude search.

2.1. Colour-magnitude and colour-colour selection

As a first cut, we set colour limits of $1.0 < (J - K_S) < 2.1$. The blue limit corresponds to a spectral type of ≈M7, while the red limit matches the reddest L dwarfs. We fit a linear relation in the (M_J, (J-K_S)) plane (Figure 1),

$$M_J \; = \; 4.2 \; (J - K_S) \; + \; 6.6, \; \sigma = 0.28 \text{ mag.}$$

and use that to eliminate source with photometric parallaxes, π_{J-K}, exceeding 83 milliarc-seconds (i.e. $d_{J-K} > 12$ parsecs). At the same time, we reject sources where the 2MASS data indicate possible contamination by diffraction spikes, diffuse emission or image artefacts (i.e. we require the 2MASS parameter $cc_flg = 000$). We have also eliminated sources where one or more of the formal uncertainties in the measured magnitudes is set to 'null', on the basis that those are likely to haver unreliable photometry.

Our use of (J, (J-K_S)) selection criteria means that we are dealing with a magnitude limited sample. As a result, Malmquist bias is introduced. The distances involved are

sufficiently small that we can assume a uniform density distribution, so the classical result applies:

$$\bar{M} \; = \; M_0 \; - \; 1.38\sigma^2 \; = \; M_0 - 0.11$$

where M_0 is the true absolute magnitude for a given (J-K_S) colour, and $\bar{M}$ the actual mean absolute magnitude in an empirically-selected sample. Near our chosen distance limit, stars with $M_J > M_0$ scatter out of the sample, while stars with $M_J < M_0$ and $d > 12$ parsecs scatter into the sample. The net effect is relatively minor: the 0.11 magnitude offset in $\bar{M}$ corresponds to an increase in the effective distance limit of only $\sim 5\%$, or $\sim 16\%$ in the effective sampling volume. Moreover, the colour-magnitude relation proves to serve more as a selection criterion than a distance estimator.

Finally, we include the (J-H)/(H-K_S) colour-colour selection criteria used to select the 2MU2 sample (Paper V). Those are designed to minimise giant contamination, while spanning the full L dwarf sequence. The resultant sample of low-latitude candidates includes $\sim 170,000$ sources - still too many for detailed follow-up.

2.2. Optical counterparts in the 2MASS catalogue

The 2MASS point-source catalogue includes optical data, primarily from the USNO-A2 catalogue (Monet *et al.*, 1998). The latter catalogue was constructed by cross-referencing scans of the POSS I blue (103aO) and red (103aE) plates with field centres north of declination -18^o, and the UKST blue (IIIaJ) and ESO red (IIIaF) plates centred at $\delta \leq -20^o$. Sources are included in USNOA2.0 only if they appear on both blue and red plates (positions coincide to better than 2 arcseconds).

A match between a 2MASS source and an object in the USNO-A2.0 catalogue requires that the positions agree to better than 5 arcseconds[1]. The average epoch of the 2MASS data is 1998, while the mean epochs are $\sim$ 1954 for POSS I and $\sim$ 1982 for UKST/ESO plate material. Thus, the requirement for positional coincidence translates to a requirement that the proper motion, μ, is less than $\sim 0.11''$ yr^{-1} for $\delta > -18^o$ and $\mu < 0.28''$ yr^{-1} for more southern sources. At 12 parsecs, those motions correspond to tangential velocities $V_{tan} < 6.25$km s^{-1} and < 16km s^{-1} , respectively. Based on the analysis in PMSU4, fewer than 3% of local disk dwarfs are expected to meet the former criterion, while only 15% meet the latter. Thus, in our search for new nearby stars, we have added the requirement that

[1]USNO was responsible for defining the 2MASS co-ordinate system, so the two catalogues have consistent astrometry.

candidates have no USNO-A2.0 optical counterpart. This reduces the target list to 70,362 sources.

2.3. IRAS sources

Since the USNO-A2 catalogue requires detection on both red and blue plates, highly-reddened late-type giants and protostars in the 2MASS database are likely to lack optical counterparts. Even though many of these objects are visible on the POSS I and ESO red plates, the enshrouding circumstellar dust leads to blue magnitudes below the limit of the 103aO or IIIaJ plate material. We can eliminate the brightest of those sources by searching for counterparts in the IRAS point source catalogue, since even the nearest late-M and L dwarfs have far-infrared fluxes well below the IRAS detection limits.

Eight thousand one hundred and thirty of our Galactic Plane nearby-star candidates lie within 60 arcseconds of an IRAS source. Figure 2 plots the number of sources as a function of positional difference, Δ. There is a strong peak at small separations, with a minimum at ~ 13 arcseconds. We have therefore excluded candidates with $\Delta < 12$ arcseconds as likely to be associated with the IRAS source. This eliminates only 1288 sources.

2.4. A candidate list of late-M/early-L dwarfs

Even after applying the above selection criteria, our list of potential nearby ultracool dwarfs still includes over 69,000 candidates. Cursory inspection of digitised sky survey data for a randomly chosen subset of these sources shows that many, probably most, are visible on at least the IVN (I-band) and the IIIaF (R-band) plates taken for the second epoch POSS II and AAO Schmidt surveys, while some are also visible on the POSS I E plate. Even with uncertainties of ± 0.25 magnitudes in the optical photometry, combining the 2MASS data with an R/I point-source catalogue would provide an effective method of eliminating a substantial fraction of the contaminating evolved giants, reddened stars and young protostars in our Galactic Plane sample. Unfortunately, such catalogues have not yet been constructed. Given those circumstances, we have modified the goals of the current investigation.

The onset of H^- absorption and pressure-induced formation of H_2 in M dwarfs leads to main-sequence stars outlining a characteristic S-curve in the (J-H)/(H-K_S) plane (as illustrated in the right-hand panel in Figure 3). Those opacity sources are much less important in low-pressure red giant atmospheres, and, as a result, those stars follow a sequence which runs above the dwarf stars (redder (J-H) colours at a given (H-K_S) (Gingerich, Latham, Linsky

& Kumar, 1966; Lee, 1970; Mould & Hyland, 1976). M-type, S-type and C-type asymptotic giant branch stars extend that sequence to redder colours, and, as Figure 3 shows, overlap with the late-M/L-dwarf sequence redward of (H-K_S) $\sim$ 0.4 magnitudes. The reddening vector (from Koorneef, 1983) is almost parallel to the giant sequence, so both protostars and distant G and K dwarfs in the Galactic Plane can lie close to the giant sequence in the JHK plane. As a result, all of these more luminous stars contaminate our colour-selected Galactic Plane sample, particularly at the redder colours corresponding to mid- and late-type L dwarfs. Therefore, for this initial study, we have defined colour limits which isolate late-type M and early-type L dwarfs:

$$\begin{aligned} (J-H) &> 1.61(H-K_S) - 0.305 \\ (J-H) &\leq 1.875(H-K_S),\ (H-K) < 0.48 \\ (J-H) &\leq 0.9,\ (H-K_S) \geq 0.48 \end{aligned}$$

All sources also have $1.0 < (J-K_S) < 2.1$.

Figure 4 illustrates how these JHK$_S$ selection criteria map onto spectral type and colour-colour distributions, plotting data for nearby stars and brown dwarfs. The primary constituents in our survey should be dwarfs with spectral types M8 to ≈L1/L1.5, although a few later-type L dwarfs (notably 2M0036+18, L3.5, Reir *et al.*, 2000) also fall within this colour range.

Applying these selection criteria reduces the list of potential nearby ultracool dwarfs from $\sim 69,000$ to only 1311 sources, including 12 duplicates. The final sample therefore includes 1299 candidates. Figure 3 plots the (J, (J-K$_S$) and (J-H)/(H-K$_S$) distribution of those sources. The concentration of candidates towards the locus occupied by red giants (and reddened main-sequence stars) is obvious in the latter diagram.

3. Results

3.1. Photographic data for the photometric sample

Having reduced the number of candidates to a manageable total, the final selection process involves examining the digitised sky survey images of each of these candidates, comparing both first and second epoch data against the 2MASS scans. To do so, we used the downloading facilities provided by CADC website (*http://cadcwww.dao.nrc.ca/dss/*). All of the first epoch images for sources at $\delta > -2^o$ are from POSS I 103aE (red) plate material (epochs 1950 to 1958); SERC/UKST IIIaJ (blue) plates provide the corresponding data for the more southern targets. POSS II supplies second-epoch IIIaF and IVN mate-

rial at $\delta > 2^o.5$, with the plates taken between 1987 and 1997, while the southern sources are covered by the SERC/UKST Galactic Plane I/SR survey. Plates for the latter survey were taken between 1977 and 1984 (Morgan, 1995), with most of the region discussed here observed in either 1979 or 1980.

What photometric characteristics are we looking for? As shown in Figure 4, ultracool dwarfs with spectral types between M7 and L2 have $5 < (R - J) < 6$. The passband of the POSS I 103aE plates overlaps with only the shorter-wavelength segment of the Cousins R-band, so these colour limits need to be adjusted. We have used Luyten's data for nearby stars (Figure 4 from Paper I) to derive the following relation,

$$(m_r - R) \ = (0.25 \pm 0.06) \ + \ (0.55 \pm 0.05)(R - I), \quad \sigma = 0.41 \text{ mag}, \ 220 \text{ stars}$$

M7 dwarfs have (R-I)$\sim$2.3 mag, and that colour saturates at $\sim$ 2.5 mag for later-type dwarfs, so the effective colour limits for the current survey are $6 < (m_r - J) < 7.5$ (allowing some latitude for intrinsic dispersion). The limiting magnitude of the POSS I 103aE platescans is $m_r \sim 20.5$, so, with $J_{max} \sim 13.5$ (Figure 3), all save the faintest candidates should be visible on the first epoch plates. However, with (B-R)$\sim$4 for ultracool dwarfs and B_J(lim)$\sim$ 22.5, a higher proportion of southern targets are likely to be absent from first epoch IIIaJ material.

Considering the second epoch plate material, the ultracool dwarfs targeted here have J$<$ 13.5 (Figure 3) and (I-J) colours in the range $2.8 < (I - J) < 4$ (Figure 4). Thus, any such objects within 12 parsecs should be detected readily on the IVN plate material ($I_{lim} \sim 18.5$). Moreover, almost all should also be visible on the IIIaF plates ($R_{lim} \sim 21.5$).

Finally, we do not expect exact positional coincidence between either first-epoch or second-epoch photographic images of genuine nearby dwarfs. The Sun has a velocity of 11 kms^{-1} with respect to the Local Standard of Rest, and the average tangential velocity of nearby disk dwarfs is $\sim$ 30 kms^{-1}. A tangential velocity of only 5 kms^{-1} produces an annual proper motion of $\sim 0.08''$ yr^{-1} at 12 parsecs. This corresponds to a displacement of $\sim$ 3.5 arcseconds between POSS I and the 2MASS imaging and $\sim$ 1.5 arcseconds between the SERC/UKST Galactic Plane survey and the 2MASS data.

In summary, genuine ultracool dwarfs within 12 parsecs are not expected to have optical counterparts at the exact 2MASS position on either the first epoch plate material or the SERC/UKST second-epoch plate material. However, those dwarfs are expected to be visible on all IVN plates and on most IIIaF and POSS I 103aE plate material. Therefore, if there is no first-epoch optical candidate at the 2MASS position, we should be able to identify an optical point-source image with no 2MASS counterpart. As discussed below, the overwhelming majority of candidates fail to meet these expectations.

3.2. The first epoch plate material

Most of the 1299 candidates can be rejected based on simple visual inspection of the first epoch plate material. Approximately half of the sample (497 sources) have an isolated, point-like optical counterpart on the first epoch images. In most cases, those sources are sufficiently red to be invisible on the blue plate material, and hence absent from the USNO catalogue. In some cases, the image is barely discernible on even the 103aE plate. The extremely red (m_r-J) colours of many of those sources fall outside the range expected for ultracool dwarfs, and suggest significant foreground (or circumstellar) reddening, while the positional coincidence with the 2MASS image argues strongly against proximity to the Sun.

In 353 cases, visual inspection shows that two (or three) stars of similar brightness, separated by < 5 arcseconds, lie at the location of the 2MASS source. It is likely that those stars are unresolved in the USNO scans of the photographic plate material, leading to incorrect co-ordinates and a failure to match one or more sources against the 2MASS database. Similarly, 311 sources lie in extremely crowded regions, mainly close to the Galactic Centre, where the high star density complicates automated analysis of the optical data. None of these candidates show evidence for significant relative motion between the first and/or second epoch DSS images and the 2MASS data. Finally, 37 sources are embedded in nebulosity on the 103aE, IIIaJ and IIIaF (but not IVN) plates.

3.3. The second epoch plate material

After eliminating all of the above spurious candidates, only 102 sources lack obvious optical counterparts on the first epoch plate material. Figure 5 plots the (α, δ) distribution of the initial 1299 sources, and the reduced sample. Almost all of the latter lie in the vicinity of the Galactic Centre, with only four sources in the northern (equatorial) hemisphere. All ninety-eight of the southern sources are covered by the UKST/SERC Galactic Plane survey, and all have R/I counterparts within 1 arcseconds of the 2MASS location on both IIIaF and IVN second-epoch plate material. As noted above, this indicates a low proper motion, $\mu < 0.06''$ yr^{-1} , corresponding to $V_{tan} < 3$ kms^{-1} for a distance of 12 parsecs. In a few cases, a very faint image is discernible on the first epoch plates (see comments in table 1); in others, the IIIaF image is substantially brighter than expected, given the absence of a clear detection on the first-epoch plate material. The last objects are probably red giant variables, which happened to have been at minimum during the initial survey observation. The absence of significant proper motion for any of these southern sources strongly suggests that all 98 are distant giants.

Of the four northern candidates, two can be ruled out as probable nearby star candidates. 2M1941443+220904 has a counterpart on the POSS II IIIaF and IVN plates, while 2M2009142+331448 is clearly visible on both POSS I and POSS II plate material, although the POSS I image is affected by a plate detect. The remaining two sources meet all our selection criteria and are confirmed as nearby dwarfs. Both have an obvious optical counterpart on the first and second epoch plate material, offset from the 2MASS source. Both targets, 2MASSI 0539248+403844 and 2MASSI 0602305+391059, have already been identified as nearby dwarfs through the Galactic Plane proper motion survey undertaken by Lépine *et al.* (2002). Lépine *et al.* (2003) estimate a spectral type of M8 for 2M0539. As part of our NStars follow-up program (described in Paper V), we obtained spectroscopy of that star (Figure 6) and estimate a spectral type of M8.5. Comparing the near-infrared photometry against data for VB 10 (M8, M_K=9.99) suggests that this star lies close to 10 parsecs distant from the Sun. 2M0602 is an early-type L dwarf at a distance of 10.6 ± 0.8 parsecs (Salim *et al.*, 2003). We also obtained spectroscopy of LSR0602 (see Salim *et al.*) and estimate a spectral type of L1.5.

4. A comparison with other surveys

Our survey of the section of the Galactic Plane covered by the 2MASS Second Incremental Release has netted only two ultracool dwarfs with photometric properties matching our selection criteria. To determine whether this meagre detection rate is reasonable, we need to compare our results against data from other surveys. We consider three comparisons: first, our own 2MASS-based survey for ultracool dwarfs at higher galactic latitudes (Paper V); second, Salim & Gould's (2003) enhanced version of Luyten's NLTT catalogue; and, finally, Lépine *et al.*'s (2002) new proper motion survey of the northern Galactic Plane.

4.1. High latitude ultracool dwarfs

Paper V describes our survey for late-type M and L dwarfs within 20 parsecs, analysing 2M2nd data covering $|b| > 10^o$. The colour/magnitude selection criteria used in this high-latitude NStars survey are broader than those used in the current survey, and only 202 of the 1672 ultracool candidates in the 2MU2 sample fall within the JHK_S limits outlined in section 2. We have either literature identifications or observations of all these sources, and the majority are red giants, predominantly drawn from the asymptotic giant branch. However, 36 objects are confirmed as late-type dwarfs, including one M4, six M5s, seven M6s, nine M7s, seven M8s, five M9s and two L dwarfs (2M0746, L0.5, and 2M0523, L2.5).

These dwarfs are drawn from 37% of the celestial sphere, so we predict an overall surface density of 6.9 ± 1.1 late-type dwarfs within the area covered by our Galactic Plane survey. Fourteen of the 36 are ultracool dwarfs, with spectral types M8 or later, so we expect a surface density of 2.6 ± 0.7 within our survey. In fact, we have succeeded in identifying one M8 and one L1.5. Thus, our results are in broad agreement with the expected numbers of M8+ ultracool dwarfs, but it seems likely that ~ 5 nearby ($d < 12$ pc.) M5 to M7 dwarfs remain to be discovered.

4.2. The Luyten surveys

Luyten's proper motion surveys provide an alternative means of identifying nearby stars. One of the main criticisms of the NLTT and LHS catalogues is the existence of substantial errors in the astrometry of a small subset of the proper motion stars. This is not really surprising, given the scope of Luyten's work and the many opportunities for transcription errors in the contemporary publishing process, and Salim & Gould (2003) point out that the overwhelming majority of stars have positions accurate to a few arcseconds. Nonetheles, the existence of these sporadic outliers complicates any statistical analysis. Fortunately, with the availability of multi-epoch digitised sky surveys, the offending stars can be re-discovered (or, in some cases, eliminated as spurious) and improved positions provided for the full catalogue. Thus, Bakos, Sahu, & Németh (2002) have used the DSS to update the LHS catalogue, while Salim & Gould have combined data from the Hipparcos, Tycho and 2MASS catalogues to similarly enhance the NLTT. We have taken the latter catalogue (designated as SGNLTT) as our primary reference here.

Salim & Gould's revised NLTT includes only systems with improved astrometry, a total of 36020 of the 58845 stars listed by Luyten. Some 28379 of those stars have 2MASS K_S-band photometry. Most of the remaining stars lie outwith the region covered by the 2M2nd, although ~ 200 are sufficiently bright that the 2MASS data are saturated. Thirty-one stars have near-infrared colours and magnitudes which meet the (J, (J-K_S)) selection criteria outlined in §2.4. As pointed out by Lépine *et al.*, four well-known late-type dwarfs, LHS 2397a, 325a, 534a and 3989a, are listed in the LHS but not the NLTT. LHS 2397a is the only star of these four which falls within the region covered by the second incremental release and, at 14 parsecs, it falls below our (J, (J-K_S)) selection criterion. Data for the SGNLTT stars are listed in Table 2 and plotted in Figure 7.

Taken at face value, Table 2 suggests that our high latitude 2MASS survey underestimates the surface density of ultracool dwarfs, particularly since seven of the 31 SGNLTT stars lie at $|b| < 10^o$ (the latter stars are plotted as solid points in Figure 7). However, many

of the sources have JHK$_S$ colours inconsistent with our selection criteria, and more detailed inspection shows that most of those stars are not ultracool dwarfs.

First, eleven of the 31 dwarfs, including 4 of the 7 stars in the Plane, are close doubles (see notes to Table 2), and the 2MASS photometry of these sources is not reliable. Optical data indicate that all are more distant, earlier-type M dwarfs. Second, visual inspection shows that the remaining three low latitude stars and LP 826-6 are incorrectly identified in the SGNLTT. In each case, the designated source shows no evidence for significant motion on the first and second epoch photographic images and the 2MASS scans; nor is there an obvious alternative candidate within 5 arcminutes. Given the JHK$_S$ colours, we identify these four SGNLTT stars as background giants, unrelated to the NLTT proper motion stars.

Five of the remaining sixteen stars are known mid-type M dwarfs: GJ 2005, GJ 3590, G180-11, GJ 3981 and Gl 866. Three of these stars meet our JHK$_S$ two-colour criteria. With spectral types between M4 and M5.5, the extremely red (J-K$_S$) colours measured for these relatively bright stars are somewhat surprising. Further investigation, particularly comparative near-infrared spectroscopy, would be interesting.

Thus, twenty of the 31 sources listed in Table 2 are not nearby ultracool dwarfs. Ten of the remaining eleven stars are included in the 2MASS photometric sample discussed in Paper V, and are confirmed as late-type dwarfs[2]. These include the M9.5 dwarf BRI0021-0214, for which 2MASS measures (J-H)= 0.94, leading to the star failing the current selection criteria. In fact, the J-band 2MASS survey image of this dwarf is affected by a meteor, and the true (J-H) colour is ~ 0.72 magnitudes (Irwin *et al.*, 1991). The final star is LHS 6234, which has (m_r-J)~ 3.9, suggesting that it is also a mid-type M dwarf with relatively red near-infrared colours.

In summary, using the NLTT catalogue to search for nearby late-type dwarfs recovers a subset of the ultracool dwarfs identified in our 2MASS NStars survey, together with a few more distant mid-type M dwarfs with unusually red near-infrared colours and one additional ultracool dwarf, BRI0021.

---

[2]We note that an additional two NLTT stars, LP 944-20 and LP 655-48, are identified as ultracool dwarfs in the 2MASS survey. LP 944-20 lies south of the $\delta = -33^o$ limit of SGNLTT; LP 655-48 is included in the SGNLTT, but an error in Luyten's proper motion precluded a match with the 2MASS data

4.3. The LSR sample

Finally, we compare our results against Lépine *et al.*'s (2002; LSR) new survey for high proper motion stars in the northern Milky Way. Taking advantage of technological advances, LSR have developed a method of aligning and differencing images from the digitised versions of the first and second epoch photographic sky surveys. Subtracting low-motion background stars greatly reduces the effective crowding, and makes it possible to use automated blink techniques to identify high-μ stars. Based on this method, LSR have identified 601 stars with $0.5 < \mu < 2.0''$ yr^{-1} , $9 < R < 20$, $|b| < 25^o$ and $\delta > 0^o$. Four hundred and sixty of those stars are catalogued by Luyten in either the LHS or NLTT, but LSR identify 141 stars as new discoveries. In fact, two of the latter stars are rediscoveries: LSR0522+38 is LP 251-35 (not included in either the LHS or NLTT); and and LSR0346+25 is WD0346+246, the archetypical cool halo white dwarf (Hambly *et al.*, 1997). Lépine, Rich & Shara (2003) have recently presented supplementary spectroscopy of a further 104 stars from this sample. Since this survey covers a significant fraction of the northern Milky Way, it provides an independent means of testing the completeness of our own photometric analysis.

Sixty-one of the 141 new proper motion stars in the LSR survey lie within the area covered by the 2M2nd, although six (all white dwarfs) are not visible on any of the 2MASS images. Of these 55 detected stars, thirty-three have $|b| < 10^o$ and overlap with the current survey. Table 3 lists the 2MASS JHK$_S$ photometry (and upper limits) for all 61 stars.

As with the Luyten stars, we can use the optical/IR photmetry to determine whether any of the LSR stars are ultracool dwarfs which should have been discovered in our survey. We can also combine the 2MASS near-infrared data with the optical photometry and astrometry measured by LSR to determine the likely nature of all of the stars in the sample, supplementing the available spectroscopy.

Figure 8 plots (J, (J-K$_S$) and (J-H)/(H-K$_S$) diagrams for the LSR sample. As before, we include data for a variety of known stellar objects to provide a reference. Inspection of these diagrams reveals several stars meeting one or other of the search criteria we have used to define our ultracool candidates. However, LSR0602 and LSR0539 are the only sources which both meet all our photometric criteria and lie within 10 degrees of the Galactic Plane.

Four other stars have (J-K$_S$) > 1.0. In two cases, the J magnitude is fainter than our selection limit, and the optical/near-infrared colours are much bluer than expected for late-type M dwarfs. These are the cool white dwarf, LSR0346+24; and LSR2105+2514, which Lowrance *et al.*(2003) have shown to be a carbon dwarf. The other two stars have more conventional colours. LSR1835+3259 has been confirmed spectroscopically as an M8.5 dwarf at a distance of less than 6 parsecs (Reid *et al.*, 2003; Lépine *et al.*, 2003), but it lies

at $b = 19^o.2$.

The fourth star, LSR0510+2713[3], is an M8 dwarf (Figure 6). However, it lies 0.02 magnitudes redder than the (J-H) upper limit of our colour selection. Increasing our selection limits to include LSR0510+2713 would add a further 1800 sources to our candidate list, more than doubling the sample size. Our spectrum of LSR0510+2713 shows emission at Hα (EW=44.5 Å) and the near-infrared calcium triplet, and the star is coincident with the X-ray source 1RXS J051019.3+271422. Comparing the photometric properties against those of VB10 suggests a distance of $\sim 8.2 \pm 1$ parsecs.

Approximately two-thirds of the 55 LSR stars have extant spectroscopy (Table 3). We can determine the nature of the remaining stars by combining the 2MASS near-infrared photometry with the observed distribution in the (R-J)/(J-K_S) two-colour diagram and the (H_R, (R-J)) reduced proper motion diagram (RPMD: Figure 9). Reduced proper motion is defined as

$$H \;=\; m + 5 + 5\log\mu \;= M \;+\; 5\log V_T \;+ const.$$

where V_T is the tangential velocity (Luyten, 1923). H can therefore serve as a surrogate for absolute magnitude, and the RPMD as an HR diagram with velocity-dependent offsets between different stellar populations.

In their analysis of the full proper motion sample, LSR considered the distribution in the (H_R, (B-R)) RPMD. This provides adequate separation between hydrogen-burning stars and white dwarfs (similar colours, but different absolute magnitudes), but is less successful in segregating late-type disk and halo subdwarfs. The disk main-sequence steepens sharply at spectral types later than ∼M2, and intersects the shallower halo subdwarf sequence at (B-R)∼ 2 (Gizis, 1997). This leads to overlapping sequences in the RPMD. The problem can be circumvented by using more appropriate colours, such as (V-I), where the two sequences both maintain a shallower slope and greater separation over a wider range of spectral types (Reid, 1997). Optical/near-infrared colours, such as (R-J), are also well suited to this type of population analysis, as highlighted by Salim & Gould (2002).

The distribution of the LSR stars in the (H_R, (R-J)) and (R-J)/(J-K_S) diagrams are shown in Figure 9. These stars have $\mu > 0.5''$ yr^{-1} , and, as a reference, we plot data for NLTT stars with similar motions (from Salim & Gould, 2003). The two-colour diagram shows that in most cases the optical/IR colours are broadly consistent with main-sequence dwarfs (the carbon dwarf, LSR2105+2514, is an obvious outlier). Three broad sequences

[3]The position listed for this star by LSR is incorrect; we measure approximate co-ordinates of $\alpha = 05:10:20.1$ $\delta = +27:14:02$ (J2000) from the DSS scans of the POSS II IVN plate.

are evident in the RPMD marking the locations of disk white dwarfs, disk main-sequence stars and, between the two disk sequences, halo subdwarfs. As an additional guide, we plot reduced proper motion data for known intermediate-abundance ($\langle [Fe/H] \rangle \sim -1$) and extremely metal-poor ([Fe/H] > -1.5) subdwarfs (from Gizis, 1997 and Reid *et al.*, 2001). Two subdwarfs, LHS 2497 and 3409 (both intermediate-abundance sdM dwarfs), lie amongst the disk dwarfs.

Based on these reference sequences, we can estimate population types for the LSR proper motion stars. Those types are listed in Table 3, together with spectroscopic data, where available. By and large, the agreement is reasonable, with LSR2010+2938 (H_R=16.85, (R-J)=0.73) the only major discrepancy: we identify it as a possible white dwarf, but spectroscopy shows it to be an early-type intermediate subdwarf. Seven LSR stars lie in the vicinity of LHS 3409 in the RPMD, and we identify those stars as possible sdM subdwarfs (labelled disk/sdM in Table 3). Spectroscopy shows that all seven are, in fact, intermediate subdwarfs.

For present purposes, the most significant aspect of Table 3 is that only 21 of the 57 LSR stars are classed as disk dwarfs. Most of those stars have colours consistent with spectral types between M3 and M6, and, therefore, $M_K < 9$ and distances exceeding 12 parsecs.

4.4. Results

Summarising the results from these comparisons, it is clear that the colour-magnitude and colour-colour limits we have adopted do not encompass the full range of properties spanned by M8 to L1.5 ultracool dwarfs. Both BRI0021-0214 (one of ten nearby NLTT dwarfs) and LSR0510+2713 (one of three LSR ultracool dwarfs) lie outwith our JHK$_S$ colour limits, although this reflects an error in the 2MASS J-band magnitude for the former star. On the other hand, the expected number densities inferred from all three comparisons are broadly consistent with observational results from the the subset of the Plane covered by the 2M2nd. In particular, almost all of the new proper motion stars identified in the LSR survey are either halo subdwarfs or mid-type M dwarfs beyond our 12-parsec limit.

5. Summary and conclusions

Based on observations of nearby dwarfs with known trigonometric parallaxes, we have developed a set of (J, (J-K$_S$)) and (J-H)/(H-K$_S$) colour-magnitude criteria designed to isolate ultracool dwarfs with spectral types in the range M8 to L3, and at distances of less than 12

parsecs from the Sun. We have applied those criteria to the Second Incremental Release of the 2MASS database, searching for candidate nearby dwarfs lying within 10 degrees of the Galactic Plane. Working from an initial sample of over 10^6 candidates with $1.0 \leq (J-K_S) < 2.1$, these criteria, combined with application of 2MASS confusion flags and elimination of candidate IRAS sources, produce a final list of 1299 potential nearby dwarfs. Visual inspection of first and second epoch photographic images form the Digitised Sky Survey shows that all save 2 of those candidates show no evidence for significant proper motion, and are therefore likely to be distant red giants or highly reddened earlier-type stars. The remaining two candidates, 2MASSI 0539248+403844 and 2MASSI 0602305+391059, are both included in Lépine *et al.*'s (2002) catalogue of new proper motion stars with $0.5 < \mu < 2.0''$ yr^{-1} in the northern Galactic Plane.

While these results are sparse statistically, the surface density is consistent with that derived for ultracool dwarfs of similar spectral types in both photometric and proper motion surveys covering higher galactic latitudes. The implication is that current estimates of the stellar luminosity function (e.g. PMSU4) are unlikely to require substantial modification to take account of a substantial reservoir of undiscovered ultracool dwarfs lying near the Galactic Plane.

However, our analysis clearly indicates potential means of improving the efficiency of photometric surveys by an order of magnitude. As discussed in §3.1, despite the significantly increased star density near the Plane, the overwhelming majority of the ultracool candidates are visible as isolated point sources on either the POSS I 103aE or SERC/UKST IIIaF/IVN plates. Matching data from those surveys directly against the 2MASS database would provide two further means of refining lists of nearby star candidates:

- First, red giants and reddened earlier-type stars generally have bluer optical/near-infrared colours than ultracool dwarfs with comparable (J-K_S) colours. The addition of R-band photometry, even with uncertainties of ± 0.25 magnitudes, should eliminate as many as 90% of the initial candidate list.

- Second, both of the photographic surveys offer sufficient baseline in time, relative to 2MASS, that proper motions can be determined to an accuracy of $0.01''$ yr^{-1} or better (equivalent to 1 km s^{-1} at 20 parsecs). Given those measurements, the remaining candidates can be prioritised in terms of their likelihood of being genuine nearby dwarfs.

The addition of these two techniques will allow us to expand our search not only to fainter magnitudes and more distant ultracool dwarfs, but also to a wider colour range, with corre-

spondingly more complete spectral type coverage[4].

As discussed above, these search methods cannot be applied to currently available databases, since the optical catalogues require detection on blue-sensitive plate material. The latter requirement is imposed with good reason, since source lists derived from scans of individual photographic plates include a substantial contribution from noise sources, generally with derived magnitudes close to the plate limit. Cross-referencing against other photographic datasets provides a means of producing a more reliable source list. Unfortunately, this practice simultaneously precludes cross-catalogue comparisons which could identify objects with extreme colours. This problem can be circumvented by integrating the complete datasets from each of these disparate surveys into a single framework which provides both access to all sources detected in a single passband, and the appropriate software tools for reliable identification of extreme-coloured, unusual sources. This clearly will be a high priority for the forthcoming National Virtual Observatory.

Thanks to K. Cruz, J. Gizis and the referee, S. Salim, for useful comments. This research was supported partially by a grant from the NASA/NSF NStars initiative, administered by Jet Propulsion Laboratory, Pasadena, CA. This research has made use of data products from the Two Micron All Sky Survey, which is a joint project of the University of Massachusetts and the Infrared Processing and Analysis Center/California Institute of Technology, funded by the National Aeronautics and Space Administration and the National Science Foundation; of the SIMBAD database, operated at CDS, Strasbourg, France; and the NASA/IPAC Infrared Science Archive, which is operated by the Jet Propulsion Laboratory, California Institute of Technology, under contract with the National Aeronautics and Space Administration.
The Digitized Sky Survey was produced at the Space Telescope Science Institute under U.S. Government grant NAG W-2166. The images of these surveys are based on photographic data obtained using the Oschin Schmidt Telescope on Palomar Mountain and the UK Schmidt Telescope. The plates were processed into the present compressed digital form with the permission of those institutions.
The National Geographic Society - Palomar Observatory Sky Atlas (POSS I) was made by the California Institute of Technology with grants from the National Geographic Society. The Second Palomar Observatory Sky Survey (POSS-II) was made by the California Institute of

[4]An alternative strategy would be to start with an LSR-style proper-motion selected sample, and then apply photometric criteria to winnow the sample size to manageable proportions. The effectiveness of this approach rests on whether digitised image subtraction can be pushed to proper motion limits of 0.1 $''$ yr^{-1} or less in crowded fields.

Technology with funds from the National Science Foundation, the National Aeronautics and Space Administration, the National Geographic Society, the Sloan Foundation, the Samuel Oschin Foundation, and the Eastman Kodak Corporation. The UK Schmidt Telescope was operated by the Royal Observatory Edinburgh, with funding from the UK Science and Engineering Research Council (later the UK Particle Physics and Astronomy Research Council), until 1988 June, and thereafter by the Anglo-Australian Observatory. The blue plates of the southern Sky Atlas and its Equatorial Extension (together known as the SERC-J), as well as the Equatorial Red (ER), the Second Epoch [red] Survey (SES) and the Galactic Plane I/SR surveywere all taken with the UK Schmidt

REFERENCES

Alonso, A., Arribas, S., & Martinez-Roger, C. 1998, A&AS, 131, 209

Bakos, G., Sahu, K. C., & Németh, P. . 2002, ApJS, 141, 187

Carpenter, J. M. 2001, AJ, 121, 2851

Cruz, K.L., Reid, I.N. *et al.*2002, AJ, subm

Dahn, C.C. *et al.* 2002, AJ, 124, 1170

Gingerich, O., Latham, D.W., Linsky, J., Kumar, S.S. 1966, in *Colloquium on late-type stars*, ed. M. Hack (Trieste), p. 291

Gizis, J. E. 1997, AJ, 113, 806

Gliese, W. & Jahreiss, H. 1991, Preliminary version of the Third Nearby Star Catalogue

Hambly, N. C., Smartt, S. J., & Hodgkin, S. T. 1997, ApJ, 489, L157

Irwin, M., McMahon, R. G., & Reid, N. 1991, MNRAS, 252, 61P

Kerschbaum, F., Lebzelter, T., & Lazaro, C. 2001, VizieR Online Data Catalog, 337, 50527

Koornneef, J. 1983, A&A, 128, 84

Lee, T. A. 1970, ApJ, 162, 217

Leggett, S. K. 1992, ApJS, 82, 351

Leggett, S. K., Allard, F., Dahn, C., Hauschildt, P. H., Kerr, T. H., & Rayner, J. 2000, ApJ, 535, 965

Lépine, S., Shara, M.S., Rich, R.M. 2002, AJ, 124, 1213

Lépine, S., Rich, R. M., & Shara, M. M. 2003, AJ, 125, 1598

Lowrance, P. J., Kirkpatrick, J. D., Reid, I. N., Cruz, K. L., & Liebert, J. 2003, ApJ, 584, L95

Luyten, W.J. 1923, *Lick Obs. Bull.*, **11**, 1

Luyten, W.J. 1979, Catalogue of stars with proper motions exceeding 0"5 annually (LHS), Univ. of Minnesota Publ., Minneapolis, Minnesota

Luyten, W.J. 1980, Catalogue of stars with proper motions exceeding 0"2 annually (NLTT), Univ. of Minnesota Publ., Minneapolis, Minnesota

Monet, D.G., et al., 1998, VizieR Online Data Catalog, 1252, The PMM USNO-A2.0 Catalogue

Morgan, D. H. 1995, ASP Conf. Ser. 84: IAU Colloq. 148: The Future Utilisation of Schmidt Telescopes, 137

Mould, J. R. & Hyland, A. R. 1976, ApJ, 208, 399

Reid, I.N., Brewer, C., Brucato, R.J., McKinley, W.R., Maury, A., Mendenhall, D., Mould, J.R., Mueller, J., Neugebauer, G., Phinney, J., Sargent, W.L.W., Schombert, J., and Thicksten, R., 1991, PASP, 103, 661

Reid, N. 1997, ASP Conf. Ser. 127: Proper Motions and Galactic Astronomy, 63

Reid, I. N., van Wyk, F., Marang, F., Roberts, G., Kilkenny, D., & Mahoney, S. 2001, MNRAS, 325, 931

Reid, I.N., Cruz, K.L. 2002, AJ, 123, 2806

Reid, I.N., Gizis, J.E., Hawley, S.L. 2002a, AJ, 124, 2721

Reid, I. N. et al. 2003, AJ, 125, 354

Salim, S. & Gould, A. 2002, ApJ, 575, L83

Salim, S. & Gould, A. 2003, ApJ, 582, 1011

Salim, S., Lépine, S., Rich, R. M., & Shara, M. M. 2003, ApJ, 586, L149

Skrutskie, M. F. et al. 1997, ASSL Vol. 210: The Impact of Large Scale Near-IR Sky Surveys, 25

This preprint was prepared with the AAS LaTeX macros v5.0.

Table 1. Ultracool dwarf candidates with $|b| < 10^o$

α (2000)	δ	J	H	K_S	Comments
5:39:24.75	40:38:43.9	11.104±0.021	10.424±0.025	10.004±0.026	confirmed M8 dwarf
6:02:30.46	39:10:59.2	12.285±0.025	11.455±0.027	10.860±0.023	confirmed L1.5 dwarf
16:09:20.92	-60:32:49.6	8.605±0.015	7.758±0.029	7.179±0.020	var?
16:57:25.54	-33:33:33.0	9.955±0.021	9.129±0.027	8.555±0.025	
17:07:33.19	-29:32:17.9	10.416±0.028	9.530±0.026	9.035±0.029	
17:08:05.91	-29:11:35.6	9.670±0.024	8.773±0.035	8.058±0.019	on 1st epoch?
17:12:40.87	-31:55:38.3	9.979±0.031	9.111±0.023	8.449±0.032	
17:12:46.01	-35:07:07.5	13.310±0.039	12.423±0.044	11.760±0.041	
17:15:22.06	-33:00:31.2	11.814±0.063	11.142±0.023	10.540±0.032	
17:19:26.84	-31:19:37.0	11.269±0.145	10.478±0.024	9.962±0.028	
17:21:55.37	-33:59:51.4	13.006±0.048	12.136±0.077	11.511±0.054	
17:24:45.66	-30:55:46.4	12.325±0.040	11.522±0.060	10.933±0.053	
17:24:56.59	-35:58:21.9	12.572±0.027	11.700±0.027	11.123±0.026	
17:25:32.08	-31:30:36.5	12.625±0.109	11.742±0.031	11.250±0.034	
17:26:02.24	-30:29:20.1	11.666±0.023	10.901±0.039	10.480±0.030	merged?
17:26:23.81	-30:44:00.9	12.689±0.015	11.808±0.038	11.286±0.036	
17:26:35.26	-35:36:48.9	12.634±0.027	11.737±0.027	11.193±0.026	
17:28:32.21	-30:55:39.4	12.346±0.043	11.628±0.093	11.013±0.079	
17:29:41.91	-31:22:17.7	12.616±0.018	11.736±0.046	11.183±0.041	
17:30:14.43	-25:40:39.9	13.557±0.038	12.668±0.063	11.977±0.045	close pair
17:31:24.00	-27:02:53.2	13.410±0.030	12.557±0.037	11.865±0.025	
17:31:29.46	-29:25:46.6	12.778±0.053	11.930±0.037	11.332±0.035	
17:31:44.28	-27:31:08.6	12.423±0.173	11.544±0.090	11.054±0.045	
17:31:46.99	-29:48:36.9	12.439±0.017	11.553±0.063	11.055±0.051	
17:31:52.59	-29:27:59.8	13.158±0.048	12.271±0.058	11.650±0.044	
17:31:57.20	-34:24:03.4	11.694±0.026	10.889±0.038	10.442±0.038	
17:33:56.56	-18:28:21.1	9.602±0.027	8.736±0.048	8.113±0.022	var?
17:35:55.62	-25:20:15.7	12.836±0.040	11.985±0.043	11.381±0.035	
17:36:07.40	-26:10:56.1	12.587±0.038	11.692±0.023	11.145±0.028	
17:36:26.86	-32:14:52.9	11.959±0.028	11.121±0.024	10.660±0.031	
17:36:36.70	-28:12:06.3	13.215±0.108	12.326±0.079	11.707±0.048	
17:36:59.86	-40:46:38.4	9.629±0.021	8.778±0.028	8.169±0.027	var?
17:38:04.74	-25:45:01.9	13.042±0.032	12.142±0.044	11.563±0.045	close pair
17:38:42.87	-31:06:08.2	13.541±0.025	12.647±0.032	11.974±0.038	
17:38:51.76	-29:16:04.8	12.384±0.030	11.583±0.044	11.078±0.050	
17:39:50.19	-30:00:40.8	12.501±0.023	11.698±0.053	11.091±0.054	
17:40:40.59	-27:56:34.5	13.347±0.048	12.459±0.055	11.752±0.048	
17:41:11.40	-27:20:00.1	13.022±0.104	12.137±0.035	11.569±0.046	
17:41:30.28	-31:06:43.6	11.912±0.031	11.026±0.030	10.493±0.041	
17:42:27.01	-30:16:33.2	12.368±0.030	11.482±0.025	10.988±0.032	
17:44:07.49	-30:39:24.9	12.336±0.024	11.467±0.026	10.957±0.032	
17:44:23.95	-26:09:19.1	13.496±0.073	12.598±0.062	11.913±0.077	
17:47:02.74	-24:50:09.1	12.693±0.097	11.922±0.059	11.332±0.055	
17:48:18.02	-25:11:47.9	11.185±0.016	10.558±0.044	10.181±0.030	
17:48:24.08	-28:18:05.6	12.629±0.021	11.737±0.037	11.255±0.030	
17:50:09.13	-36:54:59.8	9.662±0.026	8.792±0.030	8.256±0.032	on first epoch?
17:50:25.50	-39:01:18.5	10.472±0.035	9.594±0.033	9.093±0.031	
17:50:41.20	-25:17:29.4	11.757±0.025	10.857±0.026	10.229±0.037	
17:50:54.12	-31:51:14.5	11.749±0.106	11.033±0.049	10.521±0.099	

Table 1—Continued

α (2000)	δ	J	H	K_S	Comments
17:52:26.90	-25:52:50.1	12.865±0.036	11.997±0.034	11.452±0.042	
17:52:44.77	-28:06:06.1	12.294±0.031	11.486±0.038	10.904±0.044	
17:53:35.11	-22:37:36.1	13.536±0.037	12.685±0.058	11.971±0.036	
17:54:06.36	-26:16:22.9	11.755±0.027	10.950±0.034	10.398±0.040	barely visible on 1st epoch
17:54:44.05	-24:04:34.8	11.991±0.032	11.116±0.024	10.640±0.033	
17:55:01.80	-26:21:24.6	11.954±0.028	11.126±0.027	10.597±0.028	
17:56:09.80	-22:09:56.2	13.352±0.045	12.456±0.023	11.722±0.047	close pair
17:57:30.63	-23:18:37.7	12.904±0.107	12.130±0.098	11.472±0.201	
17:57:57.57	-28:04:13.4	12.983±0.051	12.101±0.074	11.517±0.053	
17:58:31.27	-24:55:17.2	13.032±0.032	12.135±0.038	11.590±0.058	
17:59:59.92	-21:18:07.5	13.378±0.048	12.504±0.231	11.855±0.052	close pair
18:00:35.95	-16:56:14.0	11.943±0.027	11.075±0.006	10.588±0.116	
18:00:51.09	-22:06:19.5	12.357±0.012	11.583±0.113	10.962±0.043	on 1st epoch
18:01:27.90	-23:27:09.4	13.075±0.027	12.236±0.034	11.616±0.032	
18:01:30.77	-35:52:11.1	10.000±0.023	9.142±0.022	8.523±0.025	
18:01:50.98	-36:59:32.9	9.618±0.023	8.742±0.012	8.181±0.012	
18:02:29.44	-22:08:55.1	12.190±0.024	11.354±0.024	10.849±0.032	
18:03:59.40	-39:55:12.3	9.568±0.029	8.756±0.022	8.137±0.031	
18:04:38.61	-16:58:18.5	13.710±0.055	12.817±0.071	12.093±0.044	
18:06:29.95	-32:54:20.3	10.154±0.024	9.317±0.025	8.846±0.027	
18:06:58.05	-16:03:51.1	13.697±0.051	12.816±0.037	12.101±0.047	
18:07:13.77	-16:52:24.8	12.761±0.067	11.892±0.055	11.321±0.046	
18:07:25.76	-20:54:14.9	12.900±0.034	12.022±0.053	11.493±0.115	
18:08:15.92	-20:08:06.7	13.060±0.046	12.193±0.028	11.483±0.037	triple
18:08:39.45	-14:18:00.5	12.585±0.096	11.735±0.040	11.209±0.016	
18:08:40.45	-30:50:14.4	9.560±0.025	8.667±0.065	8.097±0.017	
18:09:11.63	-12:30:40.8	12.182±0.025	11.431±0.043	10.923±0.013	
18:10:25.79	-33:22:36.8	10.522±0.022	9.655±0.024	9.167±0.028	
18:11:20.23	-30:23:44.6	9.962±0.023	9.089±0.021	8.552±0.027	
18:12:37.58	-19:05:34.8	12.206±0.030	11.369±0.028	10.892±0.033	
18:12:44.39	-35:41:49.0	8.913±0.015	8.019±0.051	7.437±0.015	
18:13:01.99	-18:08:49.3	10.904±0.029	10.114±0.030	9.675±0.027	
18:13:04.93	-18:08:21.4	12.115±0.030	11.301±0.029	10.833±0.027	
18:13:06.46	-17:53:42.7	11.710±0.024	10.845±0.021	10.313±0.030	
18:13:17.62	-18:06:50.9	11.787±0.025	10.997±0.021	10.564±0.030	
18:13:21.91	-17:51:36.0	10.731±0.025	9.857±0.023	9.319±0.032	
18:14:25.95	-30:35:28.7	10.553±0.021	9.743±0.035	9.300±0.028	
18:18:08.07	-35:05:39.3	9.710±0.022	8.883±0.043	8.433±0.028	
18:18:14.79	-35:22:52.8	9.768±0.030	8.986±0.029	8.410±0.029	
18:20:04.51	-24:21:55.5	9.529±0.021	8.632±0.023	8.136±0.029	
18:20:13.82	-27:09:55.9	10.018±0.028	9.164±0.022	8.597±0.029	
18:21:29.92	-26:19:10.0	9.826±0.023	8.983±0.031	8.322±0.026	on 1st epoch
18:29:13.53	-12:33:26.8	12.454±0.036	11.590±0.042	11.057±0.048	
18:37:57.35	-3:02:44.5	12.505±0.030	11.723±0.049	11.165±0.082	
18:38:57.38	-3:42:37.3	12.027±0.026	11.192±0.022	10.690±0.026	
18:39:14.55	-3:46:16.9	12.576±0.027	11.699±0.021	11.153±0.028	
18:39:30.21	-5:55:00.2	12.707±0.030	11.830±0.035	11.331±0.037	
18:39:42.51	-5:56:36.6	12.503±0.034	11.660±0.043	11.173±0.057	
18:42:22.97	-15:10:32.9	9.829±0.023	8.949±0.052	8.429±0.027	M giant

Table 1—Continued

α (2000)	δ	J	H	K_S	Comments
18:46:36.15	-18:25:21.4	10.037±0.026	9.171±0.031	8.591±0.027	
19:41:44.33	22:09:04.5	11.908±0.033	11.121±0.060	10.591±0.039	close double?
20:09:14.16	33:14:48.2	12.197±0.029	11.324±0.026	10.779±0.039	POSS I image distorted

Note. —

Table 2. Ultracool candidates from Luyten's surveys

NLTT	Name	α	δ	b	m_r	J	(J-H)	(H-K_S)	Sp. type	Sel?	Comments
1261	LP 585-86	0:24:24.6	-1:58:19	-64	19.0	12.02	0.94	0.54	M9.5	N	BRI0021
1292	LP 881-64	0:24:44.2	-27:08:24	-85	14.4	9.26	0.73	0.30	M5.5	N	GJ 2005
1470	LP 349-25	0:27:56.0	22:19:32	-40	17.0	10.61	0.64	0.41	M8	Y	Note 1
1934	LP 645-53	0:35:44.1	-5:41:10	-68	14.9	10.72	0.63	0.37	M5	Y	Note 2
3868	LP 647-13	1:09:51.2	-3:43:26	-66	17.9	11.69	0.77	0.50	M8	Y	Note 2
7395	LHS 1363	2:14:12.6	-3:57:44	-59	15.5	10.47	0.63	0.37	M6.5	Y	Note 2
13580	LP 775-31	4:35:16.5	-16:06:57	-37	17.4	10.40	0.62	0.44	M8	Y	Note 3
15886	LP 779-41	5:58:59.8	-17:28:40	-19	12.6	10.30	0.58	0.54		N	Rejected, Note 4
15887	LP 779-42	5:58:59.8	-17:28:40	-19	12.1	10.30	0.58	0.54		N	Rejected, Note 4
18549	LP 423-31	7:52:23.9	16:12:15	21	16.3	10.83	0.64	0.37	M7	Y	
20475	LP 666-9	8:53:36.2	-3:29:32	26	17.9	11.19	0.72	0.50	M8	Y	LHS 2065
23785	G 118-43	10:15:06.9	31:25:11	56	12.9	9.41	0.63	0.37	M4	Y	GJ 3590
28351	LP 375-26	11:43:37.8	24:41:25	75	12.8	11.44	0.50	1.74		N	Rejected, Note 5
30451	G 148-8B	12:21:27.1	30:38:36	83	15.0	10.26	1.01	0.40		N	Rejected, Note 6
30894	LHS 6234	12:29:09.6	62:39:38	55	14.2	10.34	0.56	0.46		Y	
33702	LP 378-1029	13:19:33.5	24:21:58	83	12.5	11.51	1.92	0.06		N	Rejected, Note 7
37621	LP 98-79	14:30:37.7	59:43:25	53	18.3	10.77	0.65	0.36	M6.5	Y	LHS 2930
38829	LP 914-54	14:56:38.3	-28:09:49	27	16.4	9.96	0.63	0.41	M7	Y	LHS 3003
41545	G 180-11	15:55:31.8	35:12:03	50	12.9	9.00	0.71	0.30	M4.5	N	G180-11
42735	LP 862-26	16:25:50.3	-24:00:08	17	15.3	11.94	0.96	0.45		N	Rejected, Note 9
43925	G 139-3	16:58:25.3	13:58:11	31	13.5	8.86	0.57	0.55	M4	Y	GJ 3981
44823	LP 920-54	17:28:24.7	-31:40:41	1	11.6	8.56	0.78	0.30		N	Rejected, Note 10
44850	LP 920-55	17:29:17.4	-30:48:37	1	11.9	11.76	1.57	0.68		N	Rejected, Note 10
45088	T 36	17:36:02.7	-30:17:58	0	16.2	9.36	1.55	0.74		N	Rejected, Note 8
45440	Ross 134	17:47:39.5	-22:56:59	2	11.9	9.75	1.31	0.23		N	Rejected, Note 11
45643	LP 921-28	17:55:21.0	-30:43:53	-3	-9.0	10.76	1.12	0.54		N	Rejected, Note 8
46471	LP 866-19	18:26:43.5	-26:18:31	-7	13.3	10.26	0.83	0.26		N	Rejected, Note 8
48781	LP 514-12	20:08:22.0	15:02:34	-10	11.6	9.50	0.88	0.17		N	G 143-33, Rejected, Note 12
54407	LP 820-64	22:38:33.6	-15:17:59	-57	12.8	6.58	0.61	0.40	M5.5	Y	Gl 866
56700	G 275-42	23:23:36.6	-22:32:16	-70	14.2	11.04	0.60	0.48	M3	Y	Rejected, Note 13
58476	-10:6203B	23:56:21.1	-9:29:57	-68	9.6	7.49	0.19	0.82		N	Rejected, Note 14

Note. — Column1 lists the record number from the SGNLTT catalogue (Salim & Gould, 2003); Column 2 gives the name, where we supplement the NLTT with designations from the Lowell survey;
Columns 3 and 4 give the 2MASS co-ordinates for equinox 2000, and column 5 lists the Galactic latitude;
Column 7 lists the red magnitude from the NLTT or LHS; Columns 8 to 10 give the 2MASS data;
Column 11 lists the spectral type, where available, and Column 12 indicates whether the (J-H)/(H-K_S) colours meet our criteria.
Notes on individual stars:
1. Catalogued by Gizis *et al.*(2002);
2. Included in Paper III of the present series;
3. Identified as a nearby star in Paper III and by Scholz *et al.*(2002);
4. Binary star with separation 5 arcseconds - 2MASS photometry unreliable;

Table 3. 2MASS data for LSR proper motion stars

Name	R	(R-J)	J	H	K_S	H_R	Class	Comments
LSR0131+5246	18.4	2.67	15.733±0.093	15.408±0.129	14.913±0.133	22.00	sd	
LSR0155+3758	14.8	4.32	10.476±0.020	9.860±0.024	9.564±0.033	18.45	disk	M5.0
LSR0157+5308	14.9	2.88	12.016±0.035	11.506±0.030	11.276±0.027	18.93	disk/sdM	sdM3.5
LSR0254+3419	19.2	···	> 17	> 16	> 15	23.95	WD	Note 1
LSR0258+5354	14.9	1.63	13.266±0.022	12.731±0.029	12.585±0.037	18.58	sd	sdK7
LSR0316+3132	15.4	3.84	11.560±0.020	10.955±0.027	10.632±0.023	19.80	disk	M5.0
LSR0346+2456	18.2	2.47	15.728±0.083	15.204±0.132	14.708±0.112	23.70	WD	Note 2
LSR0354+3333	16.4	4.60	11.799±0.031	11.270±0.032	10.886±0.022	21.04	disk	M6.0
LSR0358+8111	16.9	2.57	14.329±0.031	13.815±0.042	13.635±0.056	20.59	sd	sdM1.5
LSR0403+2616	19.1	5.60	13.503±0.031	13.041±0.036	12.698±0.035	23.22	disk	
LSR0510+2712	16.2	2.53	13.673±0.028	13.078±0.034	12.853±0.033	20.27	sd	
LSR0510+2713	15.4	4.71	10.688±0.027	9.953±0.030	9.569±0.031	19.50	disk	Note 3
LSR0519+4213	16.1	2.46	13.638±0.028	13.089±0.033	12.885±0.029	21.46	sd	esdM3.5
LSR0520+2159	16.4	1.99	14.406±0.037	13.955±0.042	13.838±0.053	20.74	sd	
LSR0521+3425	15.8	3.96	11.844±0.029	11.294±0.031	10.984±0.033	19.35	disk	M5.0
LSR0522+3814	14.5	1.36	13.143±0.030	12.744±0.039	12.622±0.035	20.66	WD	esdM3.0
LSR0524+3358	17.5	2.67	14.832±0.037	14.360±0.051	14.096±0.070	21.12	sd	sdM1.5
LSR0527+3009	16.3	4.07	12.234±0.029	11.726±0.050	11.455±0.040	20.33	disk	M5.0
LSR0532+1354	19.6	···	> 17	> 16	> 15	23.41	WD	Note 1
LSR0533+3837	16.3	2.45	13.849±0.033	13.344±0.032	13.092±0.045	20.01	sd	sdM2.0
LSR0534+2820	17.7	2.50	15.203±0.040	14.711±0.054	14.616±0.077	21.63	sd	
LSR0539+4038	17.0	5.90	11.104±0.021	10.424±0.025	10.004±0.026	22.12	disk	M8.0
LSR0541+3959	17.1	0.86	16.239±0.090	17.049±0.100	15.346±0.100	20.86	WD	
LSR0544+2603	16.1	0.28	15.820±0.075	15.240±0.107	15.110±0.134	22.25	WD	
LSR0549+2329	17.4	···	> 17	> 16	> 15	23.10	WD	Note 1
LSR0602+3910	18.3	6.01	12.285±0.025	11.455±0.027	10.860±0.023	21.89	disk	L1.5
LSR0606+1706	18.1	2.62	15.484±0.054	15.038±0.090	14.803±0.109	21.67	sd	
LSR0609+2319	16.5	3.37	13.132±0.031	12.656±0.035	12.392±0.033	21.71	disk/sdM	sdM5.0
LSR0618+1614	14.7	1.97	12.727±0.028	12.235±0.031	11.926±0.026	18.75	sd	sdM2.0
LSR0621+1219	17.3	2.61	14.693±0.042	14.410±0.055	14.337±0.091	20.85	sd	
LSR0621+3652	14.5	1.91	12.594±0.021	12.100±0.031	11.937±0.027	19.19	sd	esdK7
LSR0638+3128	19.5	4.24	15.263±0.048	14.721±0.069	14.556±0.088	23.44	disk	
LSR0646+3212	17.5	3.53	13.968±0.025	13.433±0.030	13.125±0.037	21.27	disk/sdM	M5.5
LSR0658+4442	17.4	···	> 17	> 16	> 15	22.98	WD	Note 1
LSR0702+2154	14.9	3.76	11.144±0.029	10.618±0.037	10.276±0.030	18.97	disk	M5.5
LSR0721+3714	16.2	4.40	11.802±0.035	11.128±0.048	10.835±0.037	20.04	disk	M5.5e
LSR0723+3806	19.1	···	> 17	> 16	> 15	23.70	WD	Note 1

Table 3—Continued

Name	R	(R-J)	J	H	K_S	H_R	Class	Comments
LSR0745+2627	18.4	···	> 17	> 16	> 15	23.13	WD	Note 1
LSR0803+1548	16.1	1.99	14.107±0.034	13.675±0.065	13.435±0.067	19.66	sd	sdM0.0
LSR1758+1417	15.8	0.85	14.948±0.044	14.639±0.066	14.617±0.078	20.83	WD	
LSR1809-0219	13.9	3.77	10.126±0.023	9.605±0.028	9.262±0.027	17.42	disk	M4.5
LSR1809-0247	15.2	3.80	11.399±0.021	10.911±0.029	10.674±0.026	20.21	disk	M5.0
LSR1835+3259	16.6	6.33	10.273±0.028	9.582±0.052	9.154±0.038	20.97	disk	M8.5, Note 4
LSR1922+4605	15.1	1.49	13.608±0.029	13.057±0.039	12.868±0.036	18.82	sd	sdM0.0
LSR1928-0200A	15.2	3.14	12.059±0.024	11.532±0.029	11.295±0.028	19.87	disk/sdM	M3.5
LSR1928-0200B	18.2	4.26	13.943±0.023	13.497±0.041	13.112±0.040	22.87	disk	M5.5, Note 5
LSR1933-0138	13.5	2.71	10.788±0.021	10.289±0.031	10.055±0.027	18.26	disk/sdM	M3.0
LSR1945+4650A	16.8	0.91	15.886±0.061	15.596±0.112	15.480±0.201	20.73	WD	
LSR1945+4650B	17.0	1.13	15.868±0.062	15.524±0.116	15.234±0.165	20.92	WD	
LSR2000+3057	15.6	4.95	10.648±0.030	10.113±0.034	9.706±0.019	21.23	disk	M5.5
LSR2009+5659	14.2	2.32	11.883±0.030	11.379±0.036	11.166±0.024	18.78	sd	sdM2.0
LSR2010+3938	13.3	0.73	12.567±0.027	12.084±0.030	11.842±0.022	16.85	WD?	(sd)M1.5
LSR2044+1339	15.4	4.25	11.145±0.030	10.547±0.030	10.256±0.030	18.97	disk	M5.0
LSR2105+2514	16.1	1.63	14.468±0.030	13.732±0.033	13.194±0.041	19.85	C dwarf	Note 6
LSR2107+3600	15.9	3.46	12.441±0.027	11.998±0.029	11.717±0.023	20.23	disk/sdM	M4.5
LSR2115+3804	15.0	2.05	12.953±0.028	12.469±0.029	12.253±0.025	18.52	sd	esdK7
LSR2132+4754	14.5	3.09	11.406±0.027	10.868±0.023	10.674±0.025	18.28	disk/sdM	M4.0
LSR2251+4706	17.9	4.40	13.501±0.028	12.944±0.035	12.645±0.030	21.90	disk	M6.5
LSR2311+5032	14.6	3.80	10.796±0.021	10.227±0.033	9.877±0.024	18.73	disk	M4.5
LSR2311+5103	18.1	4.85	13.254±0.023	12.684±0.032	12.289±0.026	21.73	disk	M7.5
LSR2321+4704	16.2	2.25	13.947±0.025	13.400±0.034	13.210±0.034	20.46	sd	esdM2.0s

Note. — Spectral types are taken from Lépine, Rich & Shara (2003), except for LSR0510, LSR0539, LSR0602 (this paper) and LSR1835 (Reid *et al.*, 2003).

Notes on individual objects:

1. These white dwarfs lie within the area covered by the 2MASS Second Incremental Data Release, but are not detected.
2. For further details, see Hambly *et al.*(1997).
3. LSR0510+2713 - correct position is $\alpha = 5^h10^m20^s.1, \delta = +27^o14'4''$).
4. This M8.5 dwarf lies only 5.67 parsecs from the Sun (Reid *et al.*, 2003).
5. LSR1928-0200B - correct position is $\alpha = 19^h28^m13^s.3, \delta = -2^o0'25''$).
6. Further details are given in Lowrance *et al.*(2003).

Figure captions

Fig. 1.— The (M_J, (J-K_S)) main-sequence: we plot 2MASS data for nearby M, L and T dwarfs with trigonometric parallaxes accurate to better than 10% (see Paper I and Dahn *et al.*, 2002). The solid line marks the linear colour-magnitude relation we have adopted to define the 12-parsec boundary for candidate ultracool dwarfs. Crosses mark K and M dwarfs, L dwarfs are plotted as solid points and T dwarfs as five-point stars. Note that all four L dwarfs lying over 1 magnitude above the mean relation are known near-equal luminosity binary systems. Those dwarfs are not included in the fit.

Fig. 2.— The number of 2MASS/IRAS matches as a function of the difference in position, in arcseconds. The dashed line marks a positional difference of 12 arcseconds; we assume that 2MASS sources with $\Delta \leq 12$ arcseconds are associated with the IRAS source.

Fig. 3.— The (J, (J-K_S)) and (J-H)/(H-K_S) diagrams for the surviving late-M/early-L nearby star candidates. Reference data for main-sequence dwarfs (solid squares), L dwarfs (solid points), T dwarfs (5-point stars), halo subdwarfs (from Leggett *et al.*, 2000; open circles), giants (from Alonso *et al.*, 1998; solid triangles) and Galactic AGB stars (from Kerschbaun *et al.*, 2001; open triangles) are plotted in the colour-colour diagram. Disk dwarf photometry is taken from Leggett (1992) and Dahn *et al.*(2002). The solid line shows the effect of foreground reddening of A_V=3 magnitudes. The nearby star candidates are plotted as crosses, with the dotted lines outlining the final colour-colour selection criteria.

Fig. 4.— The range of spectral types and optical/infrared colours corresponding to the (J-H)/(H-K_S) limits outlined in the text. Crosses mark data for for nearby stars and brown dwarfs; solid points identify dwarfs with colours meeting our selection criteria.

Fig. 5.— The (α, δ) distribution of the candidate ultracool dwarfs. Right ascension runs from 0 hours (left) to 24 hours (right). The upper panel plots all sources; the lower panel plots sources which really lack optical counterparts on the first epoch plate material.

Fig. 6.— Low resolution spectra of two late-type dwarfs from the LSR survey. LSR0539+40 meets the colour-magnitude criteria adopted for the current survey, and is an M8.5 dwarf at a distance of $\sim$ 10 parsecs. LSR0510+2713 lies just outwith our JHK$_S$ two-colour selection criteria, but is also an M8 dwarf at a comparable distance. A spectrum of the archetypical M8 dwarf, VB 10, is plotted for comparison.

Fig. 7.— Near-infrared colour-magnitude and colour-colour distributions of stars in the Salim/Gould NLTT catalogue which meet our (J, (J-K_S)) selection criteria. The seven dwarfs lying within 10 degrees of the Galactic Plane are plotted large solid circles the remaining

stars are plotted as crosses. The reference stars in the JHK$_S$ diagram are coded as in Figure 3.

Fig. 8.— Near-infrared data for the 55 stars in the Lépine *et al.* proper motion survey with photometry in the 2MASS Second Incremental Data Release. The solid line in the left panel marks the colour-magnitude selection criteria adopted in this survey. As discussed in the text, only four LSR stars meet those criteria. The errorbars plotted reflect the combined photometric uncertainties (from GSC2.1 and 2MASS); the reference stars in the JHK$_S$ diagram are coded as in Figure 3.

Fig. 9.— The reduced proper motion diagram and (R-J)/(J-K$_S$) two-colour diagram for LSR stars with published 2MASS photometry (solid points). The carbon dwarf, LSR2105, is circled. As a reference, we plot NLTT dwarfs with comparable motions (crosses), while the upper diagram also includes data for known intermediate- and extreme-metallicity subdwarfs (solid and open triangles, respectively). The dotted lines provide an approximate segregation between the different stellar components.

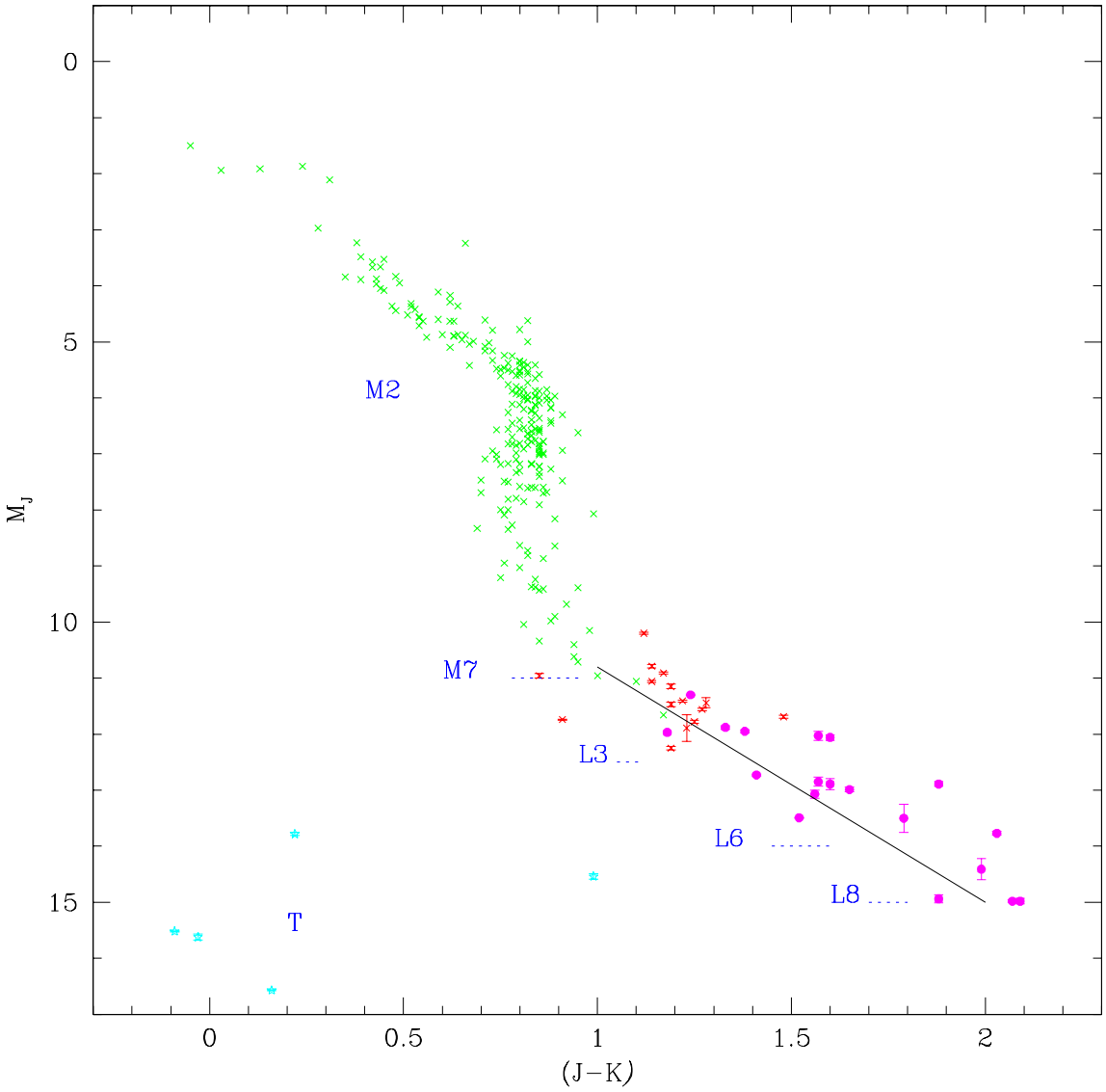

Fig. 1.— The (M_J, (J-K_S)) main-sequence: we plot 2MASS data for nearby M, L and T dwarfs with trigonometric parallaxes accurate to better than 10% (see Paper I and Dahn *et al.*, 2002). The solid line marks the linear colour-magnitude relation we have adopted to estimate photometric parallaxes for candidate ultracool dwarfs. Crosses mark K and M dwarfs, L dwarfs are plotted as solid points and T dwarfs as five-point stars. Note that all four L dwarfs lying over 1 magnitude above the mean relation are known near-equal luminosity binary systems.

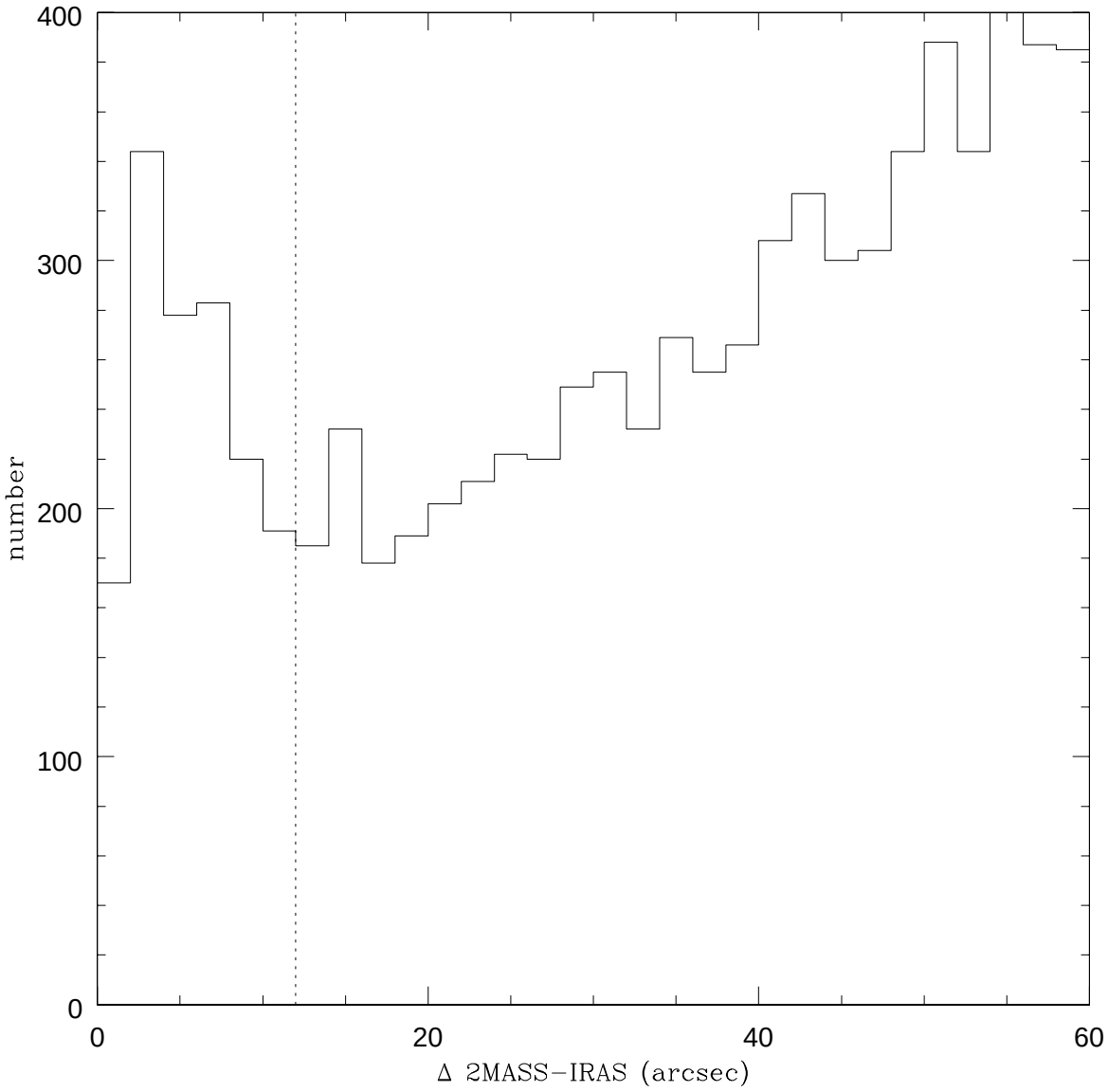

Fig. 2.— The number of 2MASS/IRAS matches as a function of the difference in position, in arcseconds. The dashed line marks a positional difference of 12 arcseconds; we assume that 2MASS sources with $\Delta \leq 12$ arcseconds are associated with the IRAS source.

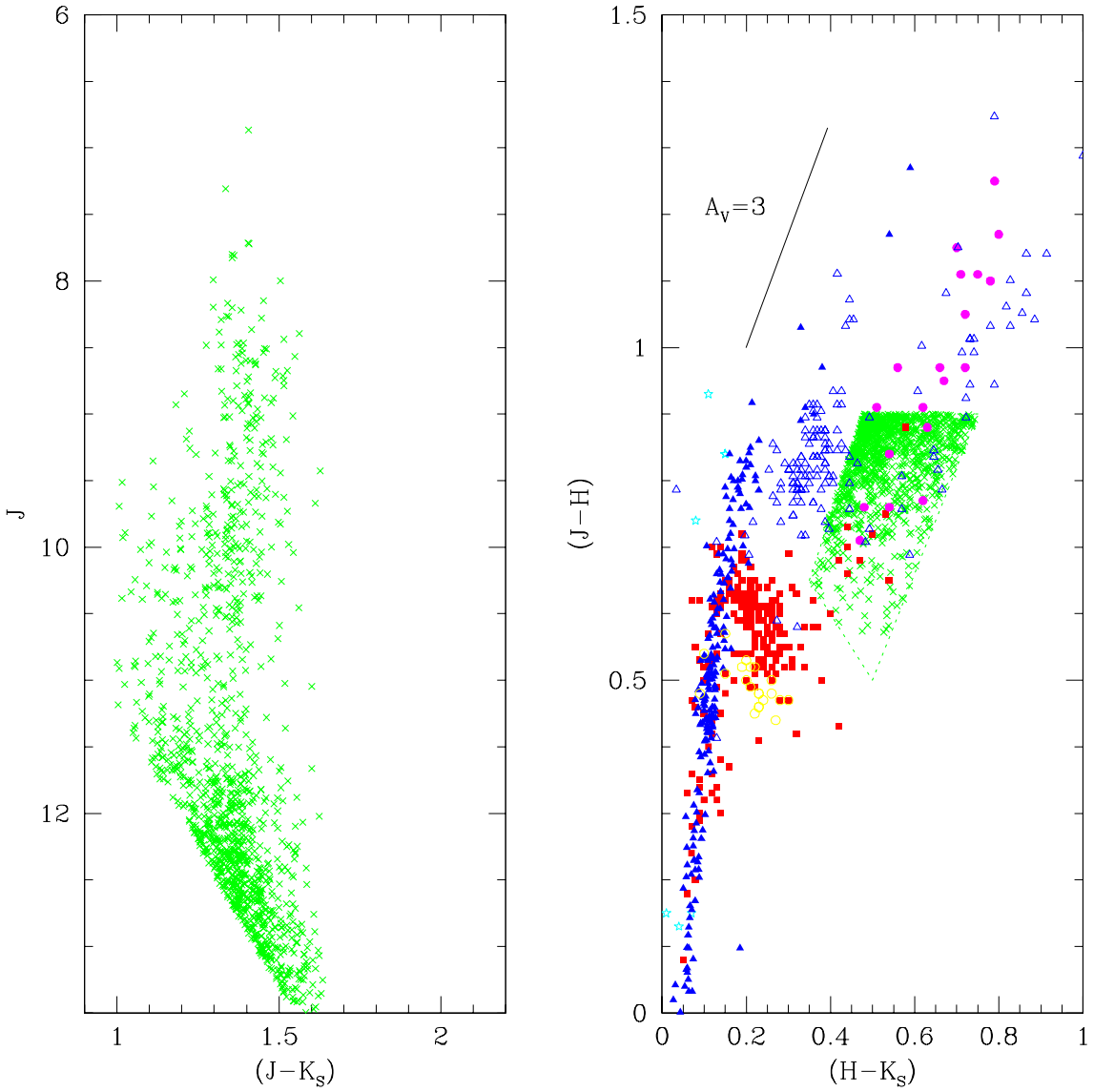

Fig. 3.— The (J, (J-K$_S$)) and (J-H)/(H-K$_S$) diagrams for the surviving late-M/early-L nearby star candidates. Reference data for main-sequence dwarfs (solid squares), L dwarfs (solid points), T dwarfs (5-point stars), halo subdwarfs (from Leggett *et al.*, 2000; open circles), giants (from Alonso *et al.*, 1998; solid triangles) and Galactic AGB stars (from Kerschbaun *et al.*, 2001; open triangles) are plotted in the colour-colour diagram. Disk dwarf photometry is taken from Leggett (1992) and Dahn *et al.*(2002). The solid line shows the effect of foreground reddening of A$_V$=3 magnitudes. The nearby star candidates are plotted as crosses, with the dotted lines outlining the final colour-colour selection criteria.

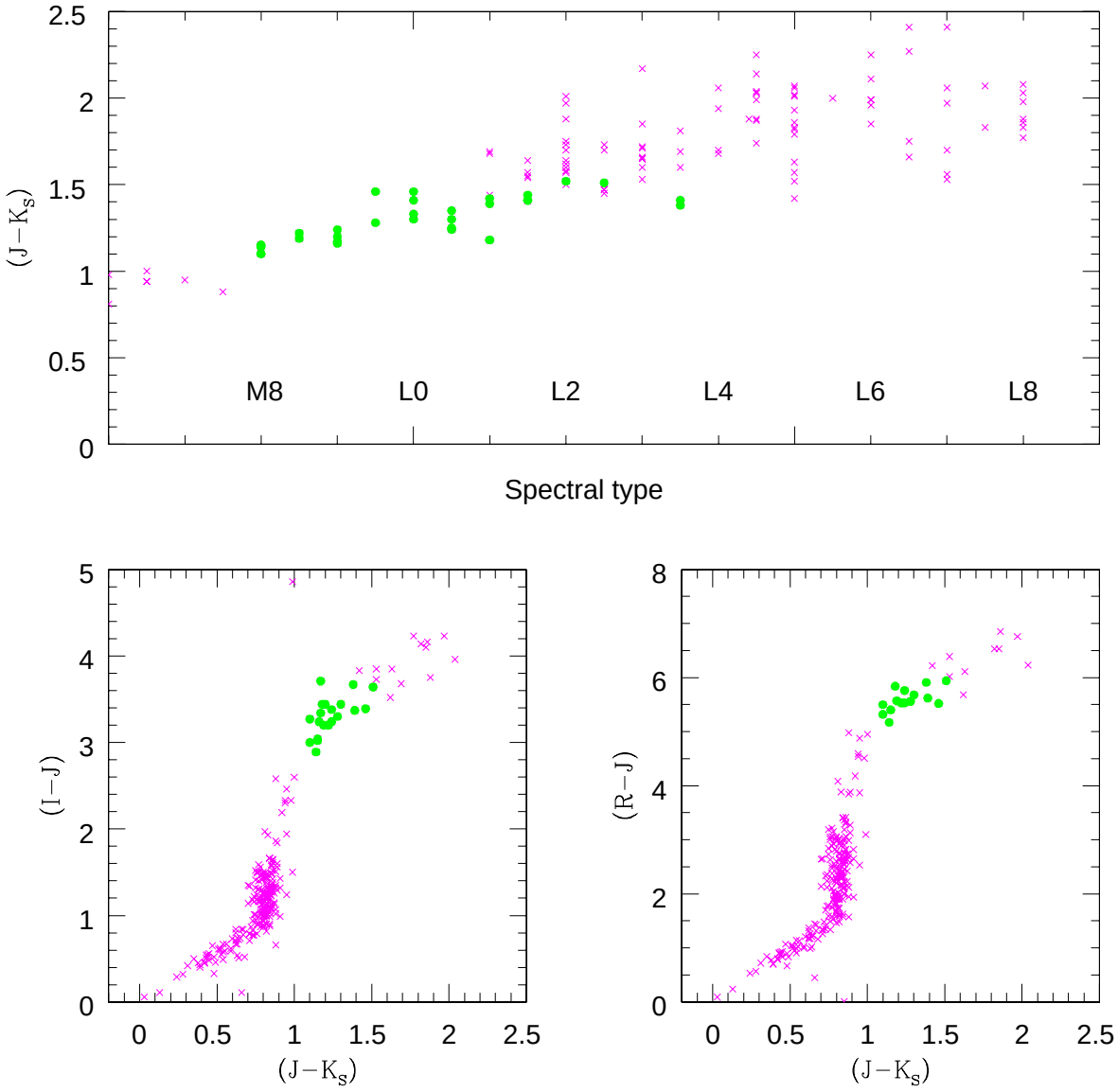

Fig. 4.— The range of spectral types and optical/infrared colours corresponding to the (J-H)/(H-K_S) limits outlined in the text. Crosses mark data for for nearby stars and brown dwarfs; solid points identify dwarfs with colours meeting our selection criteria.

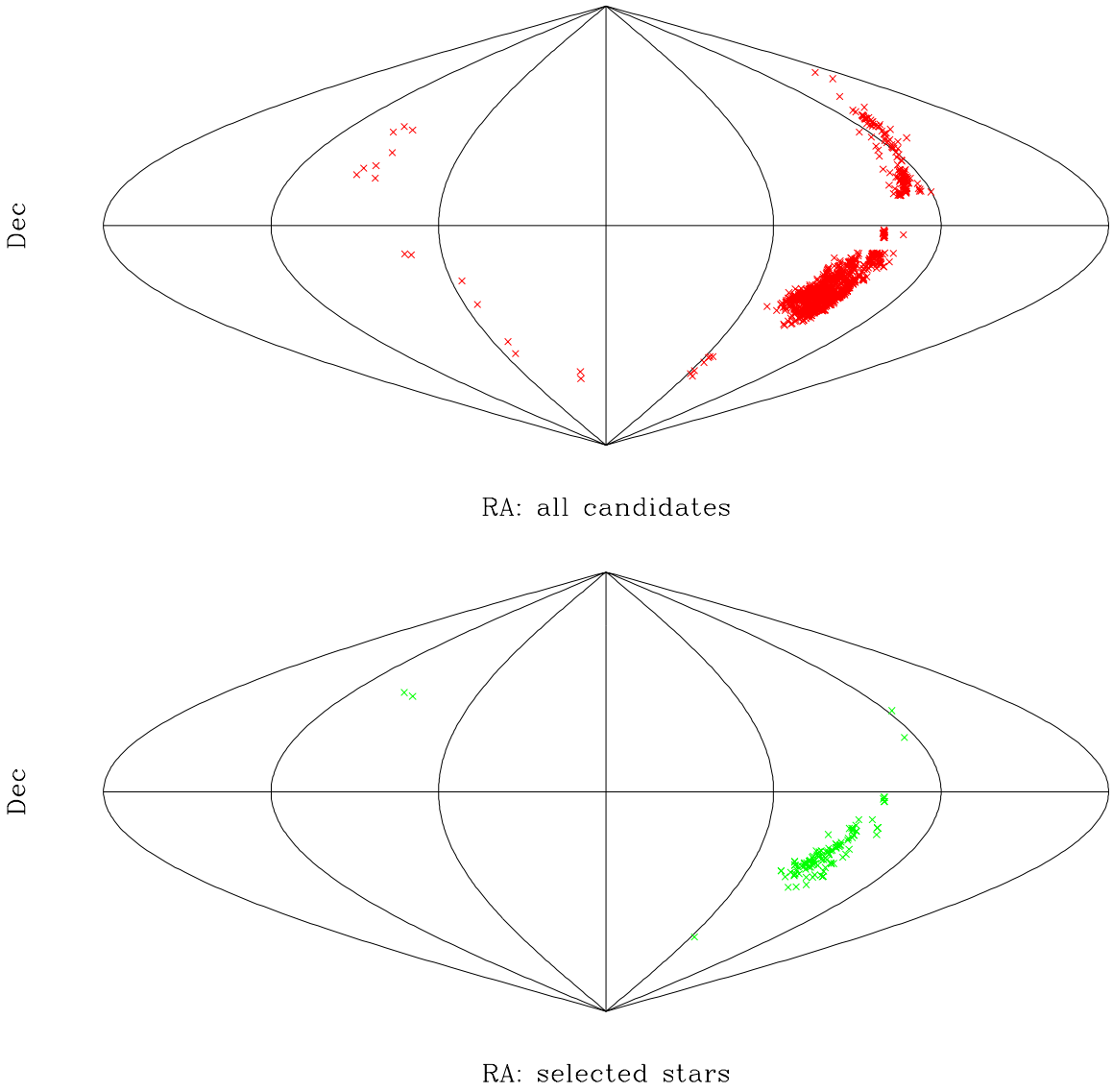

Fig. 5.— The (α, δ) distribution of the candidate ultracool dwarfs. Right ascension runs from 0 hours (left) to 24 hours (right). The upper panel plots all sources; the lower panel plots sources which really lack optical counterparts on the first epoch plate material.

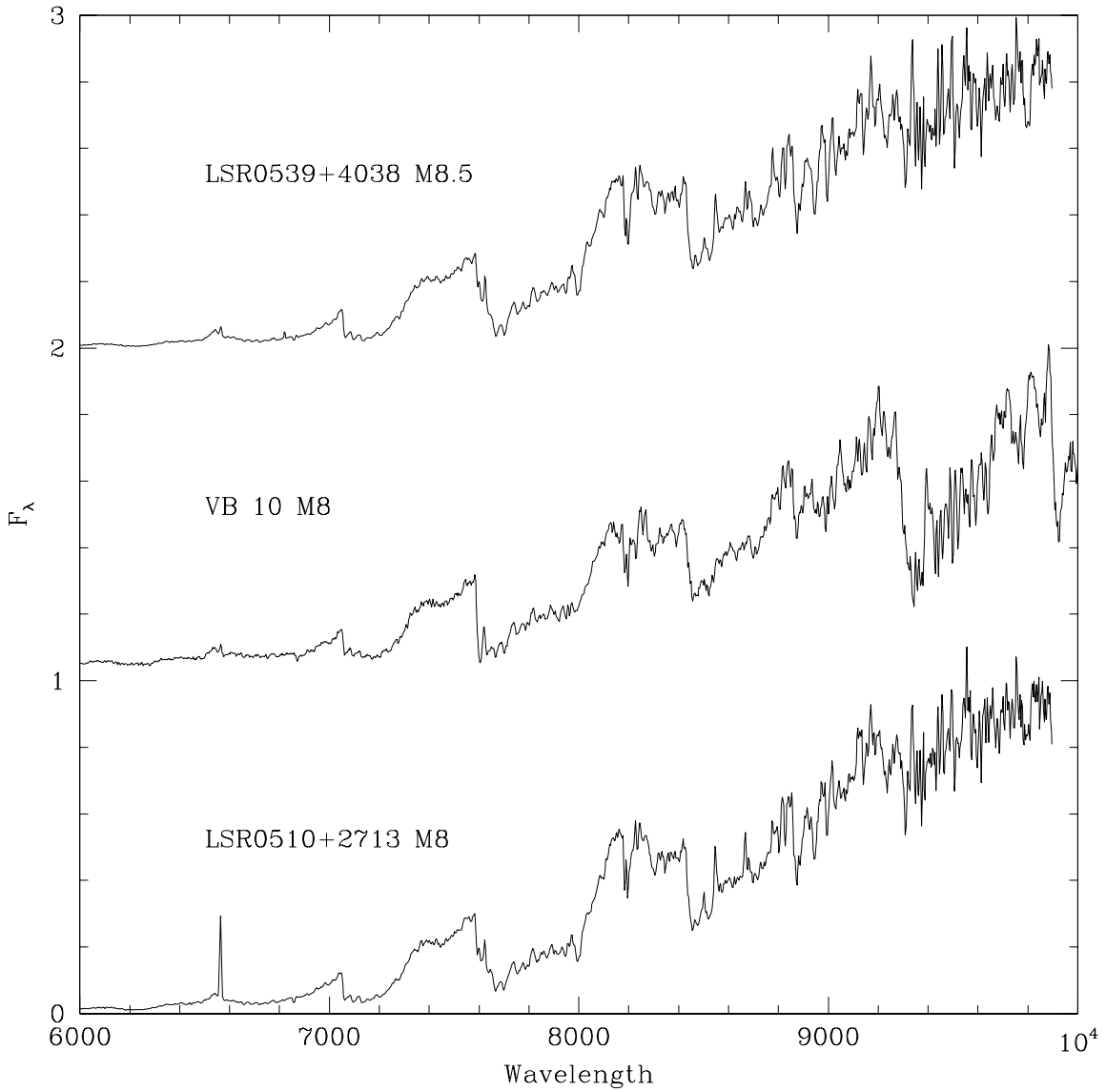

Fig. 6.— Low resolution spectra of two late-type dwarfs from the LSR survey. LSR0539+40 meets the colour-magnitude criteria adopted for the current survey, and is an M8.5 dwarf at a distance of ~ 10 parsecs. LSR0510+2713 lies just outwith our JHK$_S$ two-colour selection criteria, but is also an M8 dwarf at a comparable distance. A spectrum of the archetypical M8 dwarf, VB 10, is plotted for comparison.

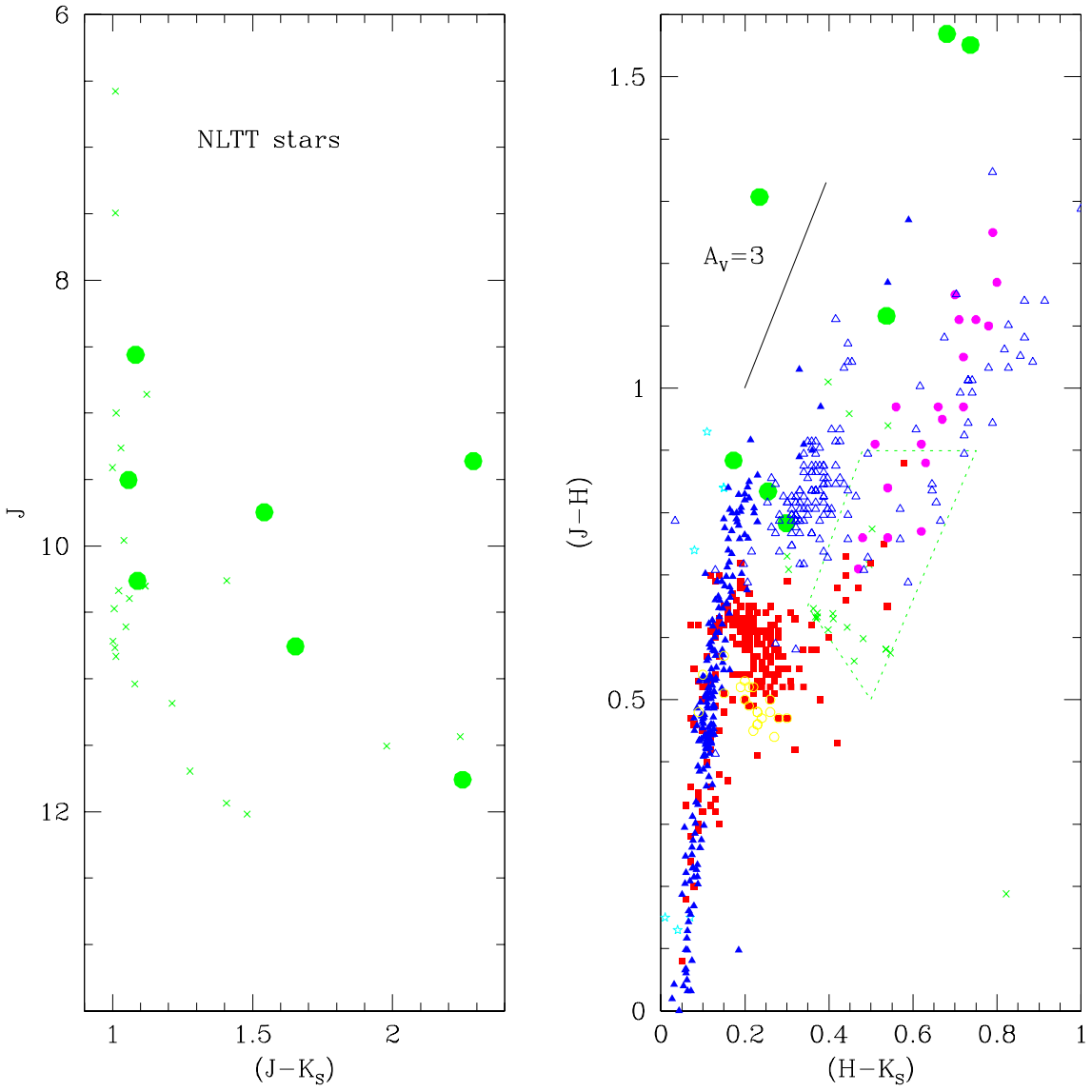

Fig. 7.— Near-infrared colour-magnitude and colour-colour distributions of stars in the Salim/Gould NLTT catalogue which meet our (J, (J-K$_S$)) selection criteria. The seven dwarfs lying within 10 degrees of the Galactic Plane are plotted large solid circles the remaining stars are plotted as crosses. The reference stars in the JHK$_S$ diagram are coded as in Figure 3.

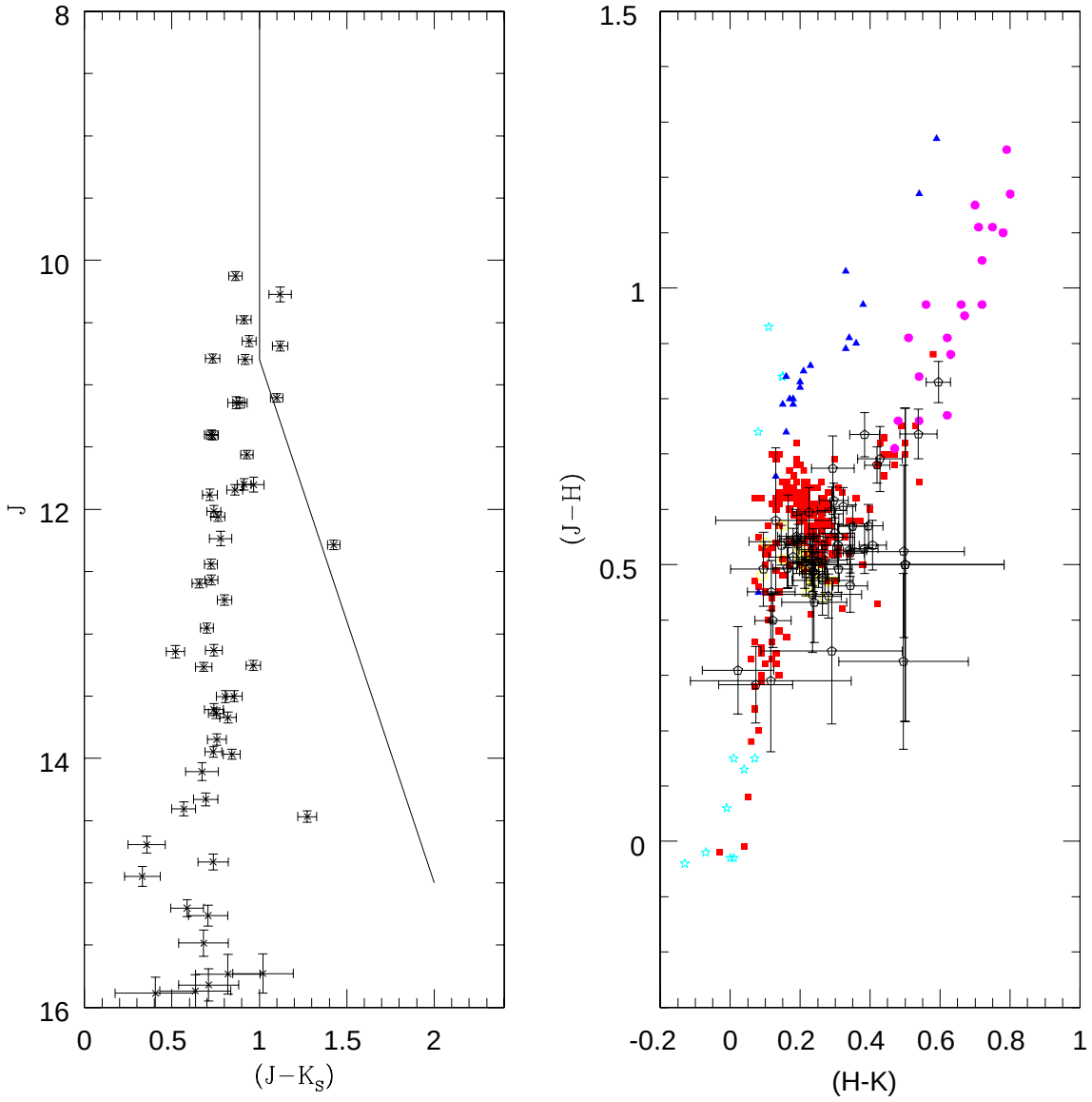

Fig. 8.— Near-infrared data for the 55 stars in the Lépine *et al.* proper motion survey which lie within the region covered by the 2MASS Second Incremental Data Release. The solid line in the left panel marks the colour-magnitude selection criteria adopted in this survey. As discussed in the text, only four LSR stars meet those criteria. The errorbars plotted reflect the combined photometric uncertainties (from GSC2.1 and 2MASS); the reference stars in the JHK$_S$ diagram are coded as in Figure 3.

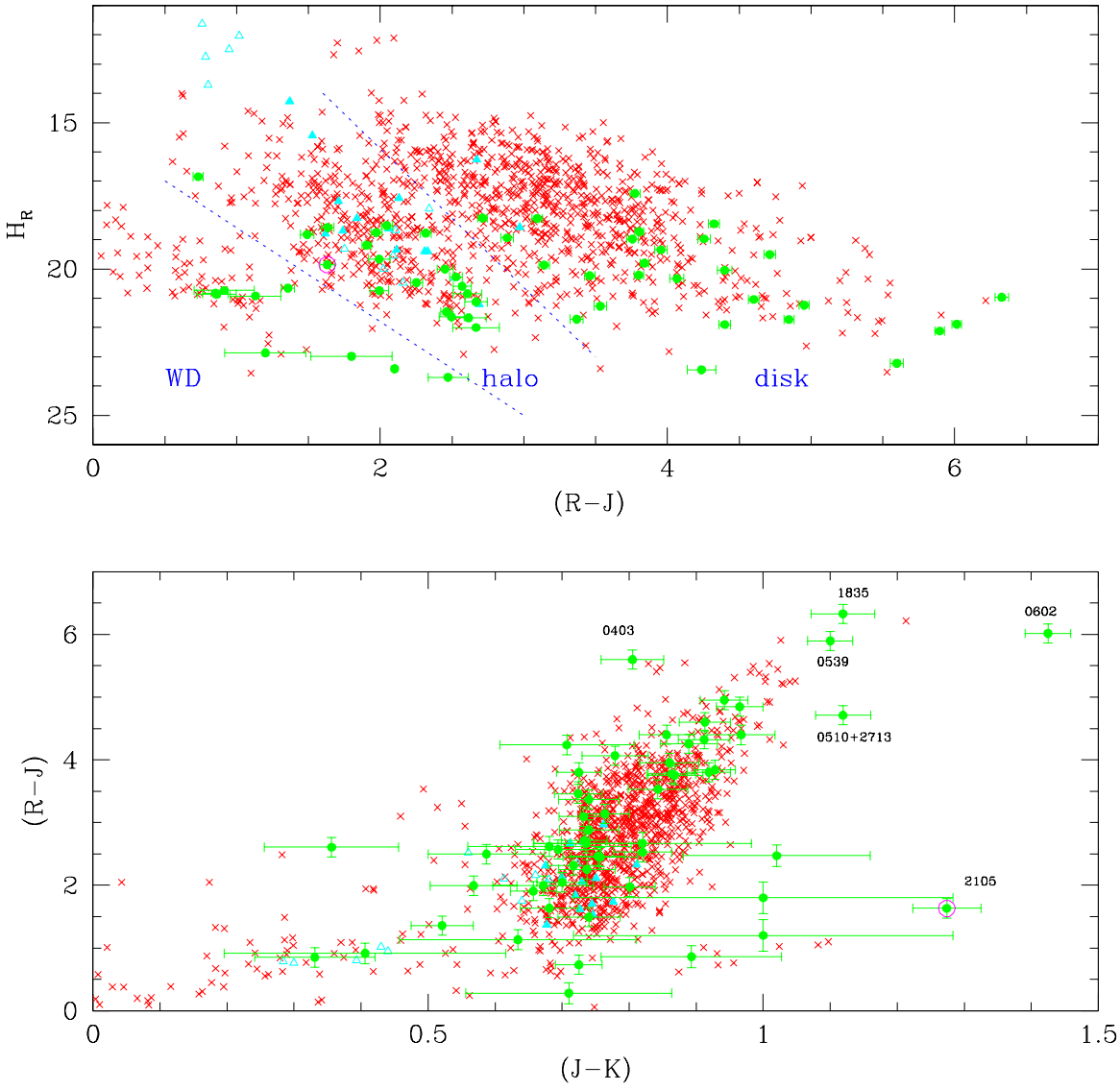

Fig. 9.— The reduced proper motion diagram and (R-J)/(J-K_S) two-colour diagram for LSR stars with published 2MASS photometry (solid points). The carbon dwarf, LSR2105, and the later-type dwarfs are identified in the two-colour diagram. As a reference, we plot NLTT dwarfs with comparable motions (crosses), while the upper diagram also includes data for known intermediate- and extreme-metallicity subdwarfs (solid and open triangles, respectively). The dotted lines provide an approximate segregation between the different stellar components.